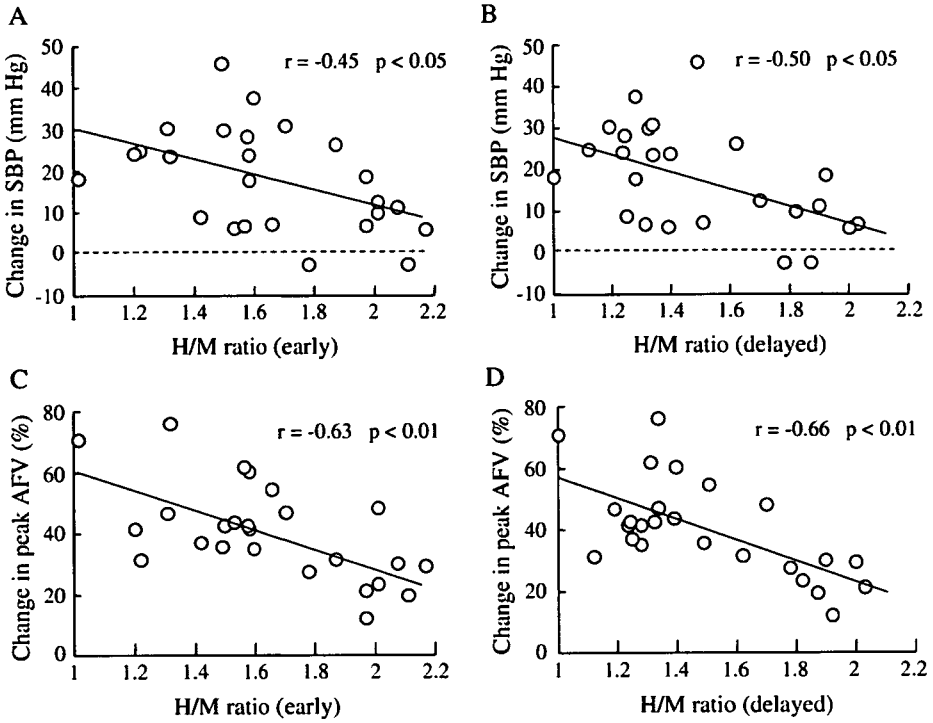

Fig. 2. Correlation between changes in SBP and peak AFV during infusion of 4 μg/kg/min DOB and the H/M ratios in patients with PD. Significant correlations between SBP changes and (A) the early image H/M ratio and (B) the delayed H/M ratio were observed. Significant correlations between changes in peak AFV and (C) early H/M ratio and (D) delayed H/M ratio were observed. SBP: systolic blood pressure, AFV: aortic flow velocity, DOB: dobutamine, PD: Parkinson's disease.

change >40 mm Hg, 1 with HR > 100/min, 1 with ventricular premature complexes, and 2 with urge to urinate). These responses were all transient and normalized within a few minutes. As many more patients experienced hyperdynamic responses after the 4 μg/kg/min dose of DOB than during the 2 μg/kg/min dose, we decided that the 4 μg/kg/min dose of DOB was the optimal dose for observing hyperdynamic cardiovascular responses.

3.2. Comparison of hemodynamic changes in control subjects and PD subjects after infusion of 4 μg/kg/min DOB

Changes from baseline in SBP, DBP, and HR are shown in Fig. 1. The increase in SBP was significantly larger in the PD patients than in the control subjects, indicating the presence of denervation supersensitivity (PD, 17.5±12.3 mm Hg; control, 7.2±6.2 mm Hg, $p<0.01$; Fig. 1A). Eleven PD patients (44%) demonstrated such a supersensitive reaction (SBP increase more than 20 mm Hg) to an infusion of 4 μg/kg/min DOB. There was also a significantly larger change in DBP in the PD subjects than in the controls (PD, 3.2±8.2 mm Hg; control, −2.8±4.5 mm Hg, $p<0.05$; Fig. 1B). There were no significant differences in the HR changes between the two groups (PD, 3.5±7.2 bpm; control, 4.3±3.6 bpm, $p=0.35$; Fig. 1C). Peak AFV increased 39.0±15.7% (range: 10.7% to 74.6%) in the PD group and 23.5±5.2% (range: 14.7 to 31.8%) in controls; the change in the PD patients being significantly larger than that in the controls ($p<0.005$; Fig. 1D).

3.3. Correlation between the MIBG H/M ratio and cardiovascular responses after infusion of 4 μg/kg/min DOB

MIBG scintigraphy was performed in all PD patients. The mean MIBG H/M ratio of the early images, obtained 15 min after injection of MIBG, was 1.65±0.31 (range: 1.02 to 2.17). Delayed images made 3–4 h later showed a mean MIBG H/M ratio of 1.49±0.30 (range: 1.00 to 2.38). Fifteen patients had H/M ratios < 1.5 in the delayed images and 10 (67%) of these patients had supersensitive reactions to 4 μg/kg/min of DOB, while 8 patients with H/M ratios > 1.7 in the delayed images all showed no supersensitive reactions. The relationships between MIBG H/M ratios and hemodynamic changes during administration of 4 μg/kg/min DOB are shown in Fig. 2. The mean increase in SBP was inversely correlated with both the early and delayed H/M ratios (Fig. 2A, B). The change in peak AFV also showed a significant negative correlation with the H/M ratios (Fig. 2C, D).

4. Discussion

This is the first study to illustrate that a hyperdynamic cardiac response due to beta1-mediated cardiac supersensitivity, assessed by an excessive increase in BP and cardiac contractility, was present during DOB infusion, and furthermore, to elucidate that this cardiac response was significantly correlated to decreased MIBG uptake in patients with PD. Decreases in the MIBG H/M ratio in PD patients represent beta-adrenergic cardiac supersensitivity, leading to

hyperdynamic cardiac contractility. This hyperdynamic cardiac contractility is not obvious under resting conditions, but does manifest itself under beta-adrenergic stress.

The presence of denervation supersensitivity is usually evaluated by observing changes in SBP or HR, and in our study SBP observation proved useful in the evaluation of cardiac sympathetic denervation. However, a hyperdynamic pressor response was not observed in about one-third of the patients who exhibited decreased MIBG uptake. This is likely to be the consequence of the influence of peripheral vascular resistance. In addition to cardiac contractility, vascular resistance also contributes considerably to SBP. DOB also has slight vasoconstriction and vasodilatation effects due to its action at alpha1- and beta2-receptors, respectively [12,13]. However, the involvement of systemic vascular resistance in the present SBP changes is not clear. There is a possibility that the increases in SBP were due to the increase of systemic vascular resistance, and that the SBP decreases were due to systemic vascular vasodilatation. Therefore, in order to more accurately evaluate the functional consequences of DOB-induced beta-receptor activation on cardiac responses, we added DOB stress echocardiography to our examination. Evaluating myocardial contractility by measuring peak AFV has certain advantages for demonstrating cardiac denervation. Peak AFV was reported to be influenced predominantly by cardiac inotropic changes [22], while the effects of physical loading are minimal [21]. Furthermore, measurement of peak AFV by Doppler ultrasound is a well-validated, noninvasive method for monitoring cardiac function [21,23]. Patients with decreased MIBG uptake demonstrated hyperdynamic AFV responses in our study. Similar hyperdynamic responses were also reported in patients with cardiac syndrome X [24]. These patients were also reported to have decreased MIBG uptake, and the presence of cardiac adrenergic nerve dysfunction was suggested [25]. These results support our findings showing a strong correlation between decreased MIBG uptake and increased cardiac contractility induced by DOB infusion. We are aware that peak AFV is not a very sophisticated measure for evaluating cardiac contractility. In general, the most frequently used, noninvasive index of left ventricular performance is ejection fraction [18]. However, to demonstrate this, a change in position, such as to the left lateral recumbent position, may be necessary, and it was expected to be difficult for PD patients to maintain such an unstable position for several minutes. Thus, to obtain a stabilized aortic waveform in the completely supine position, we carried out the evaluation from the supraclavicular fossa in our study.

Other factors may also have influenced our results. We took into consideration the influence of levodopa treatment on the cardiovascular response to DOB because hypertension, reflecting the presence of excessive amounts of catecholamines formed from levodopa, has been observed in some patients receiving the drug [26], even though the development of hypotension is much more common [27,28]. However, isoproterenol, a beta-receptor agonist resembling DOB in its action, sensitivity evaluated by a chronotropic response was similar in levodopa-treated and not-treated PD patients, and peripheral beta-adrenergic sensitivity is reported to be unaffected by levodopa treatment [29]. In addition, abnormal regurgitations (atrial, mitral, and tricuspid) are associated with ergot-derived dopamine receptor agonists [30–32]. Valvular changes may also affect the AFV monitored by DOB echocardiography. However, valvular changes are usually observed during high cumulative doses or long-term treatment with these agonists [33]. In our preliminary results, the cardiovascular responses of the patients who were never treated with levodopa or ergot-derived dopamine agonists, or were taking only 100 mg/day levodopa, were also inversely correlated with the H/M ratio (early: ΔSBP; $r=-0.64$, $p<0.05$, cardiac contractility; $r=-0.69$, $p<0.05$, delayed: ΔSBP; $r=-0.69$, $p<0.05$, cardiac contractility; $r=-0.69$, $p<0.05$) (data not shown) and these were similar to the results obtained from the full population. Together, these results seem to indicate that the cardiovascular effects of levodopa or ergot-derived dopamine receptor agonist treatment did not influence our results.

HR is generally considered a good indicator of beta1 cardiac innervation[12,13,34]. However, in only 1 of the 25 patients was it necessary to terminate the DOB procedure due to elevated HR (>100 beats/min). Overall, changes in HR were small, and during the 4 μg/kg/min infusion, there was no significant difference between the changes in PD patients and those in control subjects. At this low dose, it may be speculated that HR is accelerated by direct effects of the drug, but it is also suppressed due to a reflex cardiodeceleration secondary to the elevation in BP. Thus HR does not appear to be a proper marker for detecting beta1-receptor denervation supersensitivity with DOB.

In conclusion, our data demonstrating an exaggerated cardiovascular response to beta-adrenergic stimulation clearly confirm the pathological and nuclear medicine findings of cardiac sympathetic denervation in patients with PD. In particular, we found that a greater decrease in cardiac uptake of MIBG occurred along with a greater DOB-induced hyperdynamic response in cardiac contractility. This study documents that the beta1-adrenergic system is perturbed, and that resulting cardiac denervation is present in PD patients.

Acknowledgments

We thank the inspecting engineer Mrs. Akiko Noda and cardiologist Dr. Akira Yamada for their support with echocardiography.

References

[1] Hakusui S, Yasuda T, Yanagi T, Tohyama J, Hasegawa Y, Koike Y, et al. A radiological analysis of heart sympathetic functions with meta-[^{123}I] iodobenzylguanidine in neurological patients with autonomic failure. J Auton Nerv Syst 1994;49:81–4.

[2] Yoshita M. Differentiation of idiopathic Parkinson's disease from striatonigral degeneration and progressive supranuclear palsy using iodine-123 meta-iodobenzylguanidine myocardial scintigraphy. J Neurol Sci 1998;155:60–7.

[3] Satoh A, Serita T, Seto M, Tomita I, Satoh H, Iwanaga K, et al. Loss of ^{123}I-MIBG uptake by the heart in Parkinson's disease: assessment of cardiac sympathetic denervation and diagnostic value. J Nucl Med 1999;40:371–5.
[4] Hamada K, Hirayama M, Watanabe H, Kobayashi R, Ito H, Ieda T, et al. Onset age and severity of motor impairment are associated with reduction of myocardial ^{123}I-MIBG uptake in Parkinson's disease. J Neurol Neurosurg Psychiatry 2003;74:423–6.
[5] Kline RC, Swanson DP, Wieland DM, Thrall JH, Gross MD, Pitt B, et al. Myocardial imaging in man with I-123 meta-iodobenzylguanidine. J Nucl Med 1981;22:129–32.
[6] Orimo S, Ozawa E, Oka T, Nakade S, Tsuchiya K, Yoshimoto M, et al. Different histopathology accounting for a decrease in myocardial MIBG uptake in PD and MSA. Neurology 2001;57:1140–1.
[7] Orimo S, Oka T, Miura H, Tsuchiya K, Mori F, Wakabayashi K, et al. Sympathetic cardiac denervation in Parkinson's disease and pure autonomic failure but not in multiple system atrophy. J Neurol Neurosurg Psychiatry 2002;73:776–7.
[8] Hirayama M, Hakusui S, Koike Y, Ito K, Kato T, Ikeda M, et al. A scintigraphical qualitative analysis of peripheral vascular sympathetic function with meta-[^{123}I]iodobenzylguanidine in neurological patients with autonomic failure. J Auton Nerv Syst 1995;53:230–4.
[9] Orimo S, Ozawa E, Nakade S, Sugimoto T, Mizusawa H. (123)I-metaiodobenzylguanidine myocardial scintigraphy in Parkinson's disease. J Neurol Neurosurg Psychiatry 1999;67:189–94.
[10] Senard JM, Valet P, Durrieu G, Berlan M, Tran MA, Montastruc JL, et al. Adrenergic supersensitivity in parkinsonians with orthostatic hypotension. Eur J Clin Invest 1990;20:613–9.
[11] Niimi Y, Ieda T, Hirayama M, Koike Y, Sobue G, Hasegawa Y, et al. Clinical and physiological characteristics of autonomic failure with Parkinson's disease. Clin Auton Res 1999;9:139–44.
[12] Tuttle RR, Mills J. Dobutamine: development of a new catecholamine to selectively increase cardiac contractility. Circ Res 1975;36:185–96.
[13] Ruffolo RR. The pharmacology of dobutamine. Am J Med Sci 1987;294:244–8.
[14] Beregovich J, Bianchi C, D'Angelo R, Diaz R, Rubler S. Haemodynamic effects of a new inotropic agent (dobutamine) in chronic cardiac failure. Br Heart J 1975;37:629–34.
[15] Sawada SG, Segar DS, Ryan T, Brown SE, Dohan AM, Williams R, et al. Echocardiographic detection of coronary artery disease during dobutamine infusion. Circulation 1991;83:1605–14.
[16] Barasch E, Wilansky S. Dobutamine stress echocardiography in clinical practice with a review of the recent literature. Tex Heart Inst J 1994;21:202–10.
[17] Neskovic AN, Otasevic P. Stress-echocardiography in idiopathic dilated cardiomyopathy: instructions for use. Cardiovasc Ultrasound 2005;3:3.
[18] Gorcsan J, Deswal A, Mankad S, Mandarino WA, Mahler CM, Yamazaki N, et al. Quantification of the myocardial response to low-dose dobutamine using tissue Doppler echocardiographic measures of velocity and velocity gradient. Am J Cardiol 1998;81:615–23.
[19] Goldstein DS, Holmes C, Li ST, Bruce S, Metman LV, Cannon RO. Cardiac sympathetic denervation in Parkinson disease. Ann Intern Med 2000;133:338–47.
[20] Gibb WR, Lees AJ. The relevance of the Lewy body to the pathogenesis of the idiopathic Parkinson's disease. J Neurol Neurosurg Psychiatry 1988;51:745–52.
[21] Hsieh KS, Chang CK, Chang KC, Chen HI. Effect of loading conditions on peak aortic flow velocity and its maximal acceleration. Proc Natl Sci Counc Repub China B 1991;15:165–70.
[22] Singer M, Allen MJ, Webb AR, Bennett ED. Effects of alterations in left ventricular filling, contractility, and systemic vascular resistance on the ascending aortic blood velocity waveform of normal subjects. Crit Care Med 1991;19:1138–45.
[23] Huntsman LL, Stewart DK, Barnes SR, Franklin SB, Colocousis JS, Hessel EA. Noninvasive Doppler determination of cardiac output in man. Clinical validation. Circulation 1983;67:593–602.
[24] Madaric J, Bartunek J, Verhamme K, Penicka M, Van Schuerbeeck E, Nellens P, et al. Hyperdynamic myocardial response to beta-adrenergic stimulation in patients with chest pain and normal coronary arteries. J Am Coll Cardiol 2005;46:1270–5.
[25] Lanza GA, Giordano A, Pristipino C, Calcagni ML, Meduri G, Trani C, et al. Abnormal cardiac adrenergic nerve function in patients with syndrome X detected by [^{123}I]metaiodobenzylguanidine myocardial scintigraphy. Circulation 1997;96:821–6.
[26] Watanabe AM, Parks LC, Kopin IJ. Modification of the cardiovascular effects of L-dopa by decarboxylase inhibitors. J Clin Invest 1971;50:1322–8.
[27] Wolf JP, Bouhaddi M, Louisy F, Mikehiev A, Mourot L, Cappelle S, et al. Side-effects of L-dopa on venous tone in Parkinson's disease: a leg-weighing assessment. Clin Sci (Lond) 2006;110:369–77.
[28] Bouhaddi M, Vuillier F, Fortrat JO, Cappelle S, Henriet MT, Rumbach L, et al. Impaired cardiovascular autonomic control in newly and long-term-treated patients with Parkinson's disease: involvement of L-dopa therapy. Auton Neurosci 2004;116(1-2):30–8.
[29] Durrieu G, Rispail Y, Chatelut E, Berlan M, Rascol A, Montastruc JL, et al. Beta-adrenergic sensitivity in Parkinson's disease: effect of levodopa treatment. Clin Neuropharmacol 1990;13:492–9.
[30] Van Camp G, Flamez A, Cosyns B, Goldstein J, Perdaens C, Schoors D. Heart valvular disease in patients with Parkinson's disease treated with high-dose pergolide. Neurology 2003;61:859–61.
[31] Van Camp G, Flamez A, Cosyns B, Weytjens C, Muyldermans L, Van Zandijcke M, et al. Treatment of Parkinson's disease with pergolide and relation to restrictive valvular heart disease. Lancet 2004;363:1179–83.
[32] Zanettini R, Antonini A, Gatto G, Gentile R, Tesei S, Pezzoli G. Valvular heart disease and the use of dopamine agonists for Parkinson's disease. N Engl J Med 2007;356:39–46.
[33] Yamamoto M, Uesugi T, Nakayama T. Dopamine agonists and cardiac valvulopathy in Parkinson disease: a case-control study. Neurology 2006;67:1225–9.
[34] Baser SM, Brown RT, Curras MT, Baucom CE, Hooper DR, Polinsky RJ. Beta-receptor sensitivity in autonomic failure. Neurology 1991;41:1107–12.

THE JOURNAL OF BIOLOGICAL CHEMISTRY VOL. 282, NO. 38, pp. 28087–28095, September 21, 2007

Disulfide Bond Mediates Aggregation, Toxicity, and Ubiquitylation of Familial Amyotrophic Lateral Sclerosis-linked Mutant SOD1*[S]

Received for publication, May 31, 2007, and in revised form, July 13, 2007 Published, JBC Papers in Press, July 31, 2007, DOI 10.1074/jbc.M704465200

Jun-ichi Niwa[‡§], Shin-ichi Yamada[‡], Shinsuke Ishigaki[‡], Jun Sone[‡], Miho Takahashi[‡], Masahisa Katsuno[‡], Fumiaki Tanaka[‡], Manabu Doyu[‡§], and Gen Sobue[‡1]

From the [‡]Department of Neurology, Nagoya University Graduate School of Medicine, 65 Tsurumai-cho, Showa-ku, Nagoya 466-8500 and the [§]Stroke Center, Aichi Medical University, Aichi 480-1195, Japan

Mutations in the Cu/Zn-superoxide dismutase (*SOD1*) gene cause familial amyotrophic lateral sclerosis (ALS) through the gain of a toxic function; however, the nature of this toxic function remains largely unknown. Ubiquitylated aggregates of mutant SOD1 proteins in affected brain lesions are pathological hallmarks of the disease and are suggested to be involved in several proposed mechanisms of motor neuron death. Recent studies suggest that mutant SOD1 readily forms an incorrect disulfide bond upon mild oxidative stress *in vitro*, and the insoluble SOD1 aggregates in spinal cord of ALS model mice contain multimers cross-linked via intermolecular disulfide bonds. Here we show that a non-physiological intermolecular disulfide bond between cysteines at positions 6 and 111 of mutant SOD1 is important for high molecular weight aggregate formation, ubiquitylation, and neurotoxicity, all of which were dramatically reduced when the pertinent cysteines were replaced in mutant SOD1 expressed in Neuro-2a cells. Dorfin is a ubiquityl ligase that specifically binds familial ALS-linked mutant SOD1 and ubiquitylates it, thereby promoting its degradation. We found that Dorfin ubiquitylated mutant SOD1 by recognizing the Cys[6]- and Cys[111]-disulfide cross-linked form and targeted it for proteasomal degradation.

Cu/Zn superoxide dismutase (SOD1),[2] a major intracellular antioxidant enzyme, metabolizes superoxide radicals to molecular oxygen and hydrogen peroxide (1, 2). Because mutations in *SOD1* linked to familial amyotrophic lateral sclerosis (ALS) were first identified (3), more than 100 mutations at over 70 residues in the 153-amino acid SOD1 protein have been reported (4). Most mutations are missense mutations, with a few causing early termination or frame shifts near the carboxyl terminus of the protein. *SOD1* mutations account for ~20% of familial ALS, which is characterized by selective degeneration of motor neurons. SOD1 is primarily a cytosolic protein (5), and the active enzyme is a homodimer of two subunits (6). Each subunit contains four cysteine (Cys) residues at positions 6, 57, 111, and 146. An intramolecular disulfide bond between Cys[57] and Cys[146] of each subunit facilitates its correct folding and stabilizes the active homodimeric structure (7, 8), but it is not known how the disulfide is formed in the reducing environment of the cytosol. Although the endoplasmic reticulum is the specialized site for oxidative folding (9), there is no SOD1 localization to the endoplasmic reticulum (10). Most familial ALS-linked mutations render SOD1 more susceptible to intramolecular disulfide bond reduction (11) and accelerate the rate of protein turnover (12, 13). Recent lines of evidence implicate the disulfide-reduced monomer as the common aggregation-prone, neurotoxic intermediate of mutant SOD1 proteins (8, 11, 14–16), and a significant fraction of the insoluble SOD1 aggregates in the spinal cord of mutant SOD1 transgenic mice contains high molecular weight species cross-linked via intermolecular disulfide bonds (17). Hence, modulation of disulfide bond formation may be important in mutant SOD1-linked motor neuron-selective neurotoxicity.

ALS-linked mutant SOD1 proteins are turned over more rapidly than wild-type SOD1, and proteasome inhibitors increase the amount of mutant SOD1 (18, 19). To date, two distinct ubiquityl ligases, Dorfin and NEDL1, have been reported to ubiquitylate mutant SOD1 (20, 21). Dorfin is a RING-finger/IBR (in-between ring-finger) domain-containing ubiquityl ligase, which we previously identified from human spinal cord (22), and belongs to the RBR (RING-Between rings-RING) family of proteins (23). Dorfin physically binds and ubiquitylates various familial ALS-linked SOD1 mutants and subsequently targets them for proteasomal degradation, but it has no effect on the stability of wild-type SOD1 (20). Overexpression of Dorfin protects neuronal cells against the toxic effects of mutant SOD1 and reduces the number of aggregates composed of mutant SOD1 (20). However, the mechanism by which Dorfin discriminates between the normal and pathogenic status of SOD1 proteins remains unknown. There are numerous variants causing familial ALS, thus it seems reasonable that Dorfin recognizes a common protein modification among mutant SOD1s that is not present in wild-type SOD1.

* This work was supported by a Center of Excellence grant from the Ministry of Education, Culture, Sports, Science and Technology and grants from the Ministry of Health, Labor and Welfare of Japan. The costs of publication of this article were defrayed in part by the payment of page charges. This article must therefore be hereby marked "*advertisement*" in accordance with 18 U.S.C. Section 1734 solely to indicate this fact.

[S] The on-line version of this article (available at http://www.jbc.org) contains supplemental Fig. S1.

[1] To whom correspondence should be addressed. Tel.: 81-52-744-2385; Fax: 81-52-744-2384; E-mail: sobueg@med.nagoya-u.ac.jp.

[2] The abbreviations used are: SOD1, superoxide dismutase 1; ALS, amyotrophic lateral sclerosis; 2-ME, 2-mercaptoethanol; WST-1, 4-[3-(4-iodophenyl)-2-(4-nitrophenyl)-2H-5-tetrazolio]-1,3-benzene disulfonate; GFP, green fluorescent protein.

In this study, we generated SOD1 proteins with various combinations of the four Cys residues replaced by serines and assessed their disulfide bond status, the changes in the formations of their high molecular weight species, and their neurotoxicity. Moreover, by studying the interaction between Dorfin and these engineered SOD1s, we investigated whether disulfide bonds are critical for Dorfin recognition and ubiquitylation of mutant SOD1s.

EXPERIMENTAL PROCEDURES

Construction of Expression Vectors—Construction of pcDNA3.1/MycHis-SOD1, pEGFP-N1-SOD1, and pcDNA4/HisMax-Dorfin vectors were described previously (20, 22). Cys to Ser missense mutations were introduced into pcDNA3.1/MycHis-SOD1 and pEGFP-N1-SOD1 with a QuikChange site-directed mutagenesis kit (Stratagene, La Jolla, CA). Primer pairs for each Cys to Ser mutant were as follows: 5′-CGAAGGCCGTGTCCGTGCTGAAGGGC-3′ and 5′-GCCCTTCAGCACGGACACGGCCTTCG-3′ for C6S; 5′-GATAATACAGCAGGCTCTACCAGTGCAGGTCC-3′ and 5′-GGACCTGCACTGGTAGAGCCTGCTGTATTATC-3′ for C57S; 5′-CTCAGGAGACCATTCCATCATTGGCCGCAC-3′ and 5′-GTGCGGCCAATGATGGAATGGTCTCCTGAG-3′ for C111S; and 5′-GGAAGTCGTTTGGCTTCTGGTGTAATTGGGATCG-3′ and 5′-CGATCCCAATTACACCAGAAGCCAAACGACTTCC-3 for C146S. Multiple Cys to Ser replaced vectors were obtained by repeatedly applying a mutagenesis.

Cell Culture, Transfection, and Antibodies—Neuro-2a cells (American Type Culture Collection, Manassas, VA), a line derived from mouse neuroblastoma, were maintained in Dulbecco's modified Eagle's medium containing 10% fetal calf serum, 5 units/ml penicillin, and 50 μg/ml streptomycin. Transfections were performed using Lipofectamine 2000 (Invitrogen) in the WST-1 assay or Effectene Transfection Reagent (Qiagen, Valencia, CA) in other experiments according to the manufacturers' instructions. To inhibit cellular proteasome activity, cells were treated with 1 μM (except as otherwise indicated) MG132 (Z-Leu-Leu-Leu-al, Sigma) or epoxomicin (Sigma) as indicated concentration for 24 h after overnight transfection. To differentiate Neuro-2a cells, they were changed to Dulbecco's modified Eagle's medium culture medium containing 2% fetal calf serum and 20 μM retinoic acid and cultured for 48 h. Primary antibodies used were as follows: anti-Myc mouse monoclonal antibody (9E10, Sigma), anti-Myc rabbit polyclonal antibody (A-14, Santa Cruz Biotechnology, Santa Cruz, CA), anti-SOD1 rabbit polyclonal antibody (SOD100, Stressgen Bioreagents, Victoria, Canada), anti-α-tubulin mouse monoclonal antibody (B-5-1-1, Sigma), anti-ubiquitin mouse monoclonal antibody (4PD1, Santa Cruz Biotechnology), and anti-Xpress mouse monoclonal antibody (Invitrogen).

Transgenic Mice—17-week-old symptomatic B6SJL-TgN(SOD1-G93A)1Gur ALS mice overexpressing the human mutant $SOD1^{G93A}$ (The Jackson Laboratory, Bar Harbor, ME) were used. The experimental design of this study was fully approved by the Experimental Animal Ethical Committee of the Nagoya University Graduate School of Medicine. Tissues were homogenized in 10 volumes of lysis buffer (TNE) consisting of 50 mM Tris-HCl, 150 mM NaCl, 1% Nonidet P-40, and 1 mM EDTA with a protease inhibitor mixture (Complete Mini, Roche Diagnostics, Indianapolis, IN) and centrifuged at 20,000 × *g* for 30 min at 4 °C. Supernatants were used for Western blotting analysis.

Immunoprecipitation and Western Blotting Analysis—5×10^5 cells from a 6-cm dish were lysed on ice with 1 ml of TNE lysis buffer. The lysate was centrifuged at 1,000 × *g* for 15 min at 4 °C to remove nuclei and cell debris. Denucleated cell lysates (crude fraction) were separated into supernatant (soluble fraction) and pellet fractions by centrifuging at 20,000 × *g* for 20 min at 4 °C. The pellets were lysed (insoluble fraction) with 1 ml of TNES lysis buffer consisting of 50 mM Tris-HCl, 150 mM NaCl, 1% Nonidet P-40, 2% SDS, and 1 mM EDTA with a protease inhibitor mixture (Complete Mini, Roche Diagnostics). Protein concentrations were determined with a DC protein assay kit (Bio-Rad). Immunoprecipitation from the soluble fraction was performed with 2 μg of anti-Myc or anti-Xpress antibodies and Protein A/G Plus-agarose (Santa Cruz Biotechnology), and the precipitates were washed four times in TNE buffer. Cell lysates or immunoprecipitates were separated by SDS-PAGE (5–20% gradient gel) and analyzed by Western blotting with ECL plus detection reagents (GE Healthcare Bio-Sciences, Piscataway, NJ). Non-reducing SDS-PAGE was conducted without 2-mercaptoethanol (2-ME) in the sample buffer. Because omitting reducing agents from the protein samples can lead to adventitious air oxidation or disulfide scrambling, 100 mM iodoacetamide was added to the lysates to prevent these changes during sample preparation.

Filter Trap Assay—Each of the various fractions from the cell lysates (crude, soluble, and insoluble fractions) was filtered under vacuum through 0.2-μm cellulose acetate membranes (Sartorius, Gottingen, Germany) followed by two washes in Tris-buffered saline. The membranes were then incubated with 5% milk powder in Tris-buffered saline at room temperature for 1 h, followed by an overnight incubation at 4 °C with anti-Myc antibody in Tris-buffered saline with 0.1% Tween 20. Primary antibodies were detected with horseradish peroxidase-conjugated secondary antibodies (GE Healthcare Bio-Sciences), which were then detected with ECL plus chemiluminescence reagent (GE Healthcare Bio-Sciences). To confirm equal loading of proteins, the same samples were blotted onto 0.45-μm nitrocellulose membranes (Bio-Rad) and probed with anti-Myc or anti-α-tubulin antibodies.

Neurotoxicity Analysis and Quantification of SOD1 Aggregates—2×10^4 Neuro-2a cells were grown overnight on four-chamber, collagen-coated slides (Nalge Nunc, Rochester, NY) and then transfected with 0.2 μg of pEGFP-N1-SOD1. After overnight incubation, the cells were differentiated in Dulbecco's modified Eagle's medium containing 2% fetal calf serum and 20 μM retinoic acid for 48 h. Inclusion bodies were counted in more than 100 randomly selected cells, and the percentages of cells with such inclusions were calculated. Data from three independent experiments were averaged. For the cell viability assay, 5×10^3 Neuro-2a cells were grown in 96-well collagen-coated plates overnight, and then transfected with 0.1 μg of pEGFP-N1-SOD1 or pcDNA3.1/MycHis-SOD1, with or without 0.1 μg of pcDNA4/HisMax-Dorfin. pcDNA4/HisMax

mock vector was used as a control. A 4-[3-(4-iodophenyl)-2-(4-nitrophenyl)-2H-5-tetrazolio]-1,3-benzene disulfonate (WST-1)-based cell proliferation assay (Roche Diagnostics) was performed 48 h after differentiation. Absorbance was measured in a multiple plate reader (PowerscanHT, Dainippon Pharmaceutical, Japan). The assay was carried out in triplicate and statistically analyzed by one-way analysis of variance or unpaired *t* test.

Quantitative Analysis of Gene Expression Levels—Total RNA was extracted from Neuro-2a cells expressing SOD1-GFP and their Cys to Ser derivatives by using an RNA Easy Kit (Qiagen), followed by cDNA synthesis primed with oligo(dT) using Superscript II (Invitrogen). The gene expression level was examined by quantitative reverse transcription-PCR using primer sets specific to target genes and QuantiTect SYBR Green PCR kit (Qiagen). PCR was performed on an iCycler system (Bio-Rad) under the manufacturer's recommended conditions.

Isolation of SOD1 Aggregates—Isolation of SOD1 inclusion bodies was carried out according to Lee *et al.* (24) with a slight modification. 5×10^5 Neuro-2a cells in a 60-mm dish expressing SOD1-GFP were washed with cold phosphate-buffered saline before addition of TNE buffer. After a 5-min incubation at room temperature, the supernatant containing Nonidet P-40-soluble proteins was carefully removed from dishes. After gentle washing of dishes with phosphate-buffered saline, the Nonidet P-40-insoluble materials were scraped and incubated on ice for 5 min. The extract was then centrifuged at $80 \times g$ for 15 min. The pellet containing big inclusions was put onto a slide glass, sealed with a coverslip, and observed under a BX51 epifluorescence microscope (Olympus, Tokyo, Japan).

Cycloheximide Chase Analysis—Neuro-2a cells grown on 6-cm dishes were transfected with 1 μg of pcDNA3.1/MycHis-SOD1 with or without 1 μg of pcDNA4/HisMax-Dorfin. 24 h after transfection, cycloheximide (50 μg/ml) was added to the culture medium, and the cells were harvested at the indicated time points. The samples were subjected to SDS-PAGE and analyzed by Western blotting with anti-Myc antibody. The intensities of the bands were quantified by ImageGauge software (Fuji Film, Tokyo, Japan). The assay was carried out in triplicate and statistically analyzed by one-way analysis of variance or unpaired *t* test.

RESULTS

Proteasome Inhibition Increases SDS-resistant Disulfide-linked Species as Well as Insoluble Ones of ALS-linked Mutant SOD1—Mutant SOD1 is a fairly unstable protein, and the increased turnover of mutant SOD1 is mediated by the ubiquitin-proteasome pathway (18, 19). Thus, we first examined the effect of proteasome inhibition on mutant SOD1 proteins. When cellular proteasome activity was blocked by the proteasome inhibitor MG132, the level of soluble mutant $SOD1^{G85R}$ and $SOD1^{G93A}$ increased in a dose-dependent manner (Fig. 1*B*, *arrowhead*), and an SDS-resistant mutant SOD1 dimer appeared (Fig. 1*B*, *arrow*). The increase in the amount of wild-type SOD1 was much smaller than that of mutant SOD1 (Fig. 1*B*, *arrowhead*). Detergent-insoluble, sedimentable mutant SOD1 also increased as proteasome activity was inhibited (Fig. 1*C*). Interestingly, as the proteasome activity was inhibited, aberrant high molecular weight SDS-resistant disulfide-linked mutant $SOD1^{G85R}$ and $SOD1^{G93A}$ became more abundant (Fig. 1*A*, *asterisk*). There were almost no SDS-resistant disulfide-linked species of the wild-type SOD1. The same findings were obtained when blots were probed with anti-SOD1 antibody (supplemental Fig. S1*A*). These results were also confirmed with epoxomicin, a selective and irreversible proteasome inhibitor (supplemental Fig. S1*B*). Thus, intermolecular disulfide bond-linked mutant SOD1 is unstable and prone to degradation by the proteasome.

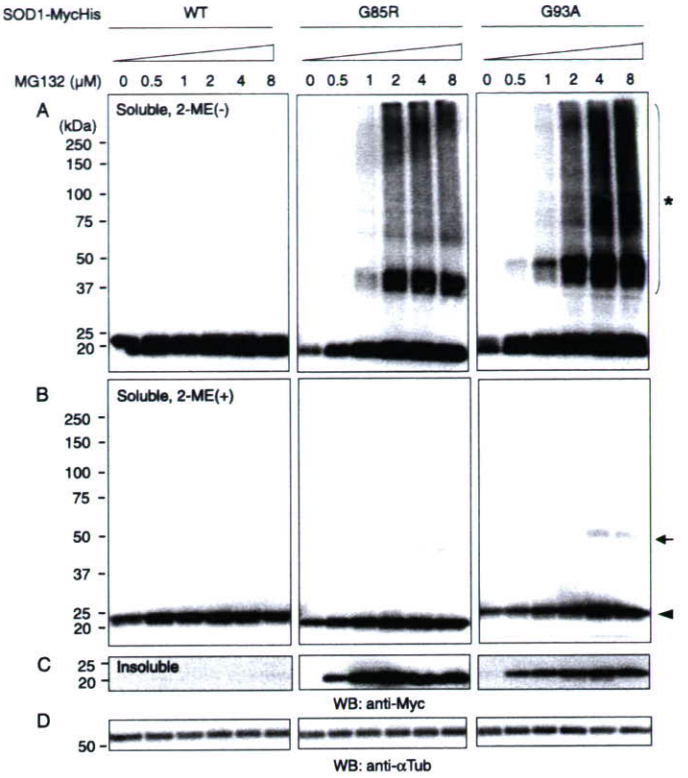

FIGURE 1. **Proteasome inhibition leads to the accumulation of intermolecular disulfide bond-linked mutant SOD1.** Neuro-2a cells expressing wild-type (*WT*), G85R, and G93A mutant SOD1-MycHis were treated with MG132 for 24 h at the indicated concentrations. Soluble fractions were analyzed by SDS-PAGE in the absence (*A*) or presence (*B*) of 2-ME. Insoluble fractions were analyzed by SDS-PAGE in the presence of 2-ME (*C*). *Arrow*, a soluble SDS-resistant dimer; *arrowhead*, a soluble monomeric SOD1; *asterisk*, disulfide-linked high molecular weight-species of SOD1. *D*, anti-α-tubulin as loading control.

Free Cys^6 and Cys^{111} Are Important for Generating Disulfide Bond-linked Species and Insoluble, Sedimentable Forms of Mutant Human SOD1—We examined the role of Cys residues in the formation of aberrant disulfide-bond linked high molecular weight species. Various combinations of the four Cys residues at positions 6, 57, 111, and 146 replaced with serines were introduced into SOD1 protein-expression vectors using site-directed mutagenesis. The effects of amino acid replacement at one of the four Cys residues, at two of the four Cys residues, and at all four Cys residues on wild-type and two familial ALS-linked SOD1 mutants, $SOD1^{G85R}$ and $SOD1^{G93A}$, were investigated. We used Myc-His-tagged SOD1 expression vectors and an antibody against the tag peptide to detect SOD1 protein so as to avoid possible reduced detection of SOD1 with multiple

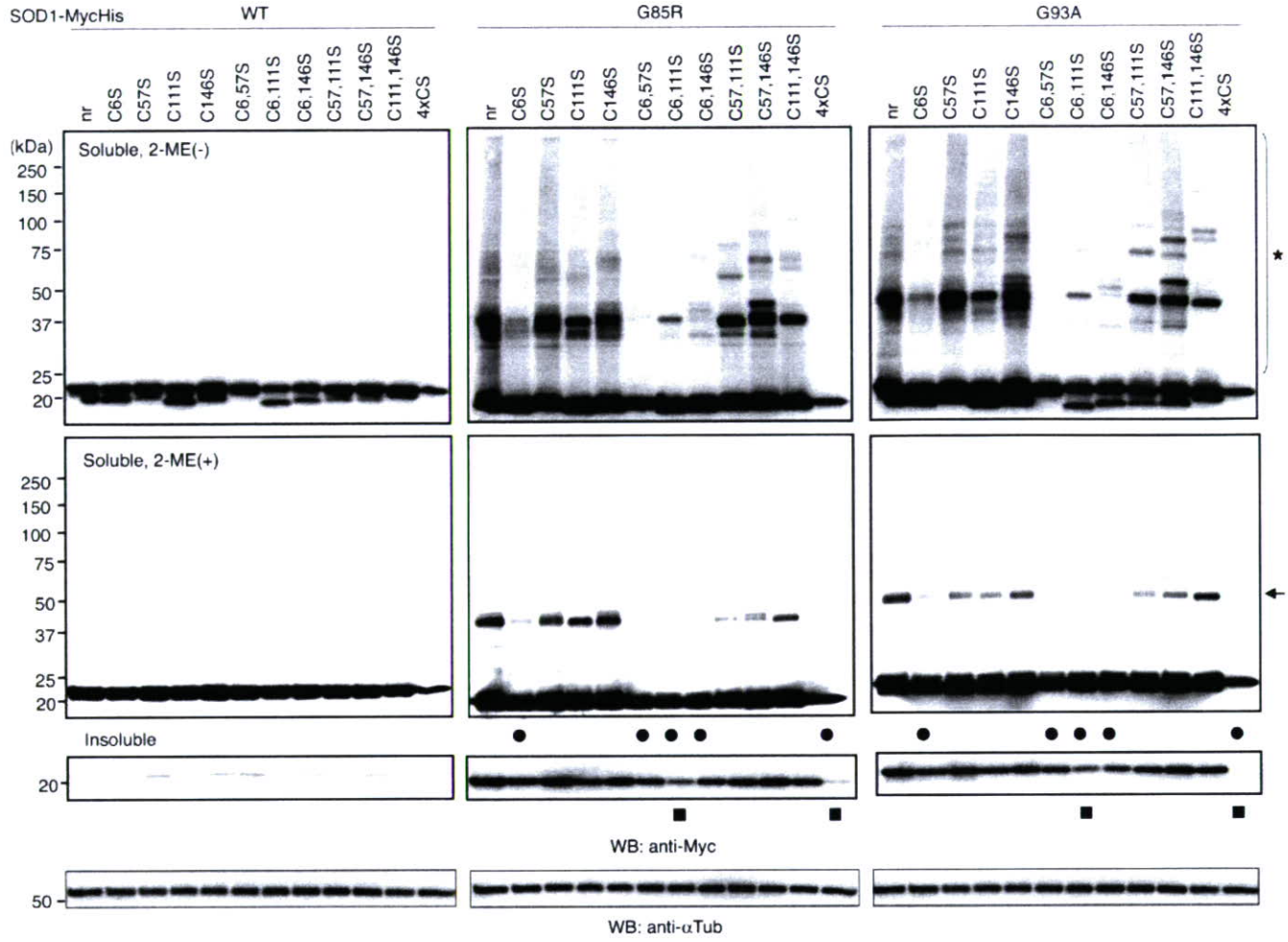

FIGURE 2. **Free Cys^6 and Cys^{111} are important for generating intermolecular disulfide-linked species and insoluble, sedimentable forms of mutant human SOD1.** Various combinations of replacing Cys with Ser were introduced into wild-type (*WT*) and mutant (G85R and G93A) SOD1-MycHis. Neuro-2a cells expressing SOD1-MycHis were treated with 2 μM MG132 for 24 h. Soluble fractions were analyzed by SDS-PAGE in the absence (*upper panels*) or presence (*middle panels*) of 2-ME. Insoluble fractions were analyzed by SDS-PAGE in the presence of 2-ME (*lower panels*). *Asterisk*, a disulfide-linked high molecular weight species; *arrow*, an SDS-resistant dimer of mutant SOD1. *Filled circles*, marked reduction of an SDS-resistant dimer with a Cys^6 replacement of mutant SOD1; *filled squares*, further reduction of the detergent-insoluble, sedimentable form of mutant SOD1 with simultaneous Cys^6 and Cys^{111} replacements. *nr*, SOD1 without replacement in cysteine residue; *4×CS*, all four cysteines replaced by serines.

amino acids changes by the anti-SOD1 antibody. Interestingly, none of the Cys residue replacements generated disulfide-linked species in wild-type SOD1 proteins (Fig. 2, *left panel*). Under reducing conditions, replacement of Cys^6 had a stronger effect on the formation of disulfide-linked species of mutant SOD1 than did the other three Cys residue replacements (Fig. 2, *middle* and *right panels*, *asterisk*). Combinations of replacing Cys^6 and one of the other Cys residues further attenuated the aberrant disulfide-linking of mutant SOD1 seen with the single substitution of Cys^6 (Fig. 2, *filled circle*). Under usual reducing conditions, the same reduced oligomerization of mutant SOD1 was observed when combinations of Cys^6 and other Cys residues were replaced (Fig. 2, *arrow*). The detergent-insoluble, sedimentable form of mutant SOD1 was also reduced especially if both Cys^6 and Cys^{111} were replaced (Fig. 2, *filled square*). Replacement of all four Cys residues completely abolished the disulfide-linked species in the non-reducing condition and the oligomeric, detergent-insoluble form of mutant SOD1 in the reducing condition (Fig. 2, *lane 4×CS*). Because simultaneous substitutions of Cys^6 and Cys^{111} had the strongest effects on the formation of aberrant species of mutant SOD1 in both non-reducing and reducing conditions, we compared C6S and C111S mutants with C57S and C146S mutants in the following experiments.

Substituting Both Cys^6 and Cys^{111} Greatly Reduces High Molecular Weight Aggregate Formation and Ubiquitylation of Mutant SOD1—In studies of polyglutamine disorders, it has been demonstrated that high molecular weight aggregates of mutant proteins are retained by filtration through cellulose acetate (25, 26). Cellulose acetate membranes usually bind protein very poorly and are used to trap high molecular weight structures from complex mixtures through filtration. This assay was also successfully applied to detect mutant SOD1 aggregation (27). Thus we used a cellulose acetate filter trap assay to investigate whether SOD1 proteins with Cys substitutions are retained in high molecular weight aggregates from lysates of SOD1-MycHis expressing Neuro-2a cells. Cells were lysed in TNE buffer, fractionated into crude denucleated, soluble, and insoluble fractions, and each fraction was then filtered through a 0.22-μm cellulose acetate membrane. Subsequent staining

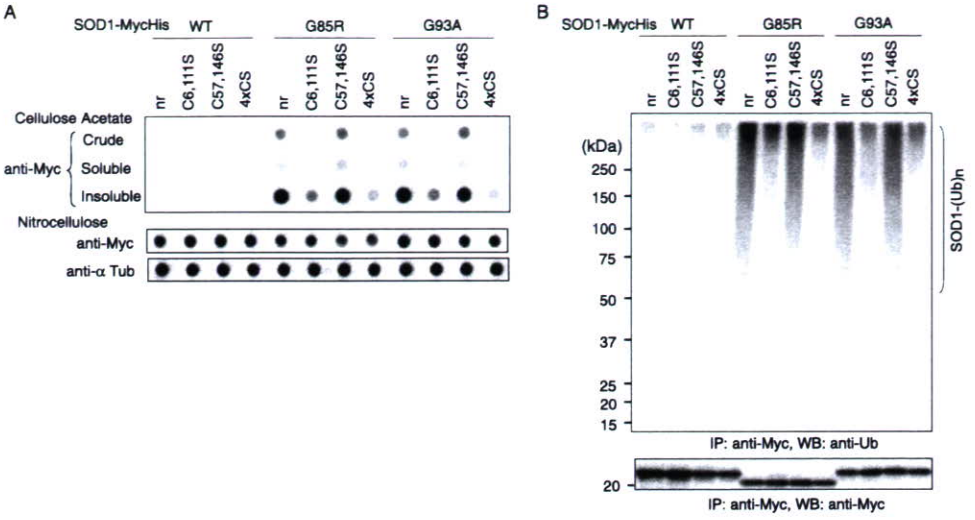

FIGURE 3. **Replacing both Cys^6 and Cys^{111} greatly reduces high molecular weight aggregate formation and ubiquitylation of mutant SOD1-MycHis.** *A*, crude, soluble, and insoluble fractions of cell lysates were analyzed by filter trap assay (*upper panel*). Nitrocellulose dot blots probed with anti-Myc (*middle panel*) and anti-α-tubulin (*lower panel*) antibodies were used as loading controls. *B*, *in vivo* ubiquitylation assay. Western blotting of SOD1-Myc-His immunoprecipitates with anti-ubiquitin antibody demonstrated polyubiquitylation of mutant SOD1s and their C57, 146S derivatives. Replacement of Cys^6 and Cys^{111} abolished polyubiquitylation of mutant SOD1. *nr*, SOD1 without replacement in cysteine residue; *4×CS*, all four cysteines replaced by serines.

with anti-Myc antibody revealed trapped SOD1 proteins (Fig. 3*A*, *upper panel*). Interestingly, high molecular weight aggregates were abundantly detected in mutant SOD1^{G85R}, SOD1^{G93A}, and their C57S and C146S derivatives. Replacements of Cys^6 and Cys^{111} greatly reduced high molecular weight structures of mutant SOD1. No high molecular weight aggregates were present in either wild-type SOD1 or their Cys-substituted mutants.

Mutant, but not wild-type, SOD1 is conjugated to a multiubiquitin chain and degraded at the proteasome (20, 28). To assess whether SOD1 proteins are ubiquitylated, we carried out an *in vivo* ubiquitylation analysis by expressing SOD1^{WT}, SOD1^{G85R}, SOD1^{G93A}, and their Cys to Ser mutants in Neuro-2a cells in the presence of the proteasome inhibitor MG132. When SOD1 was then immunoprecipitated, mutant SOD1s, but not wild-type SOD1, were polyubiquitylated (Fig. 3*B*, *lane 1*). Replacement of both Cys^6 and Cys^{111} abolished ubiquitylation of mutant SOD1, whereas replacement of Cys^{57} and Cys^{146} did not affect the ubiquitylation status of mutant SOD1 (Fig. 3*B*, *lane 2 versus lane 3*). Wild-type SOD1 and its Cys-replacement mutants were not ubiquitylated at all. Replacing only one of the four Cys residues attenuated neither the formation of high molecular weight species nor the ubiquitylation of mutant SOD1 (data not shown). Thus, the presence of both Cys^6 and Cys^{111} is important for high molecular weight aggregate formation and ubiquitylation of mutant SOD1. Disulfide bond formation at Cys^6 or Cys^{111} is critical step for ubiquitylation of mutant SOD1.

Formation of Disulfide-linked Species of Mutant SOD1 Strongly Correlates with Visible Aggregate Formation and Neurotoxicity—Expression of mutant, but not wild-type, SOD1 induces large perinuclear intracytoplasmic aggregates in differentiated Neuro-2a cells and reduces cellular viability (20). We analyzed the role of mutant SOD1 Cys residues in aggregate formation and neurotoxicity in Neuro-2a cells. Replacements of Cys^6 and Cys^{111} significantly reduced the percentage of mutant SOD1^{G85R} and SOD1^{G93A} cells with visible aggregates (Fig. 4*A*). To further demonstrate the extent of aggregate formation, we isolated SOD1 aggregates with a procedure according to Lee *et al.* (24). Differentiated Neuro-2a cells bearing SOD1-GFP aggregates were extracted with 1% Nonidet P-40 in the culture dish, and the Nonidet P-40-soluble proteins were gently removed. Under this condition, the soluble monomeric SOD1 was completely removed, and the aggregates remained in the culture dish due to their association with unknown structures (24). The remaining Nonidet P-40-insoluble portion was then scraped and centrifuged at 80 × *g*. After the centrifugation at 80 × *g* for 15 min, the pellet fraction was found to contain exclusively the large inclusion bodies. Replacements of Cys^6 and Cys^{111} markedly reduced the number of inclusion bodies in G93A mutant SOD1-GFP (Fig. 4*B*). Mutant SOD1^{G85R} and SOD1^{G93A}, but not wild-type SOD1, are toxic in differentiated Neuro-2a cells as previously described (20). However, replacement of the Cys^6 and Cys^{111} residues markedly reduced this neurotoxicity (Fig. 4*C*), which was not affected by replacing the Cys^{57} and Cys^{146} residues. There were no significant differences among the expression levels of all the constructs (Fig. 4*D*). Thus, changes in inclusion formation and toxicity are not due to differences in altered expression. These results provide evidence of direct links among intermolecular disulfide bonding, ubiquitylated complex formation, visible aggregate formation, and neurotoxicity.

Preferential Occurrence of Disulfide-cross-linked Mutant SOD1 in the Affected Lesions of ALS Model Mice—Although mutant SOD1 is expressed at similar levels in both neuronal and non-neuronal tissues, the aggregated and ubiquitylated forms are selectively found in the pathological lesions of patients and mutant SOD1-transgenic mice (29, 30). Thus, we next examined whether mutant SOD1 is aberrantly disulfide-linked in various tissues from symptomatic mutant SOD1 transgenic mice. Western blotting analysis, using anti-SOD1 antibody under reducing and non-reducing (omitting reducing agent 2-ME) conditions, demonstrated that the expression levels of mutant SOD1 were nearly the same in all tissues examined. Each of the tissues showed some of the disulfide-linked mutant SOD1species; however, in the brain stem and spinal cord, the areas predominantly affected in mutant SOD1-linked ALS, there was increased formation of intermolecular disulfide-linked species of mutant SOD1 (Fig. 5). Thus, intermolecular disulfide-linked

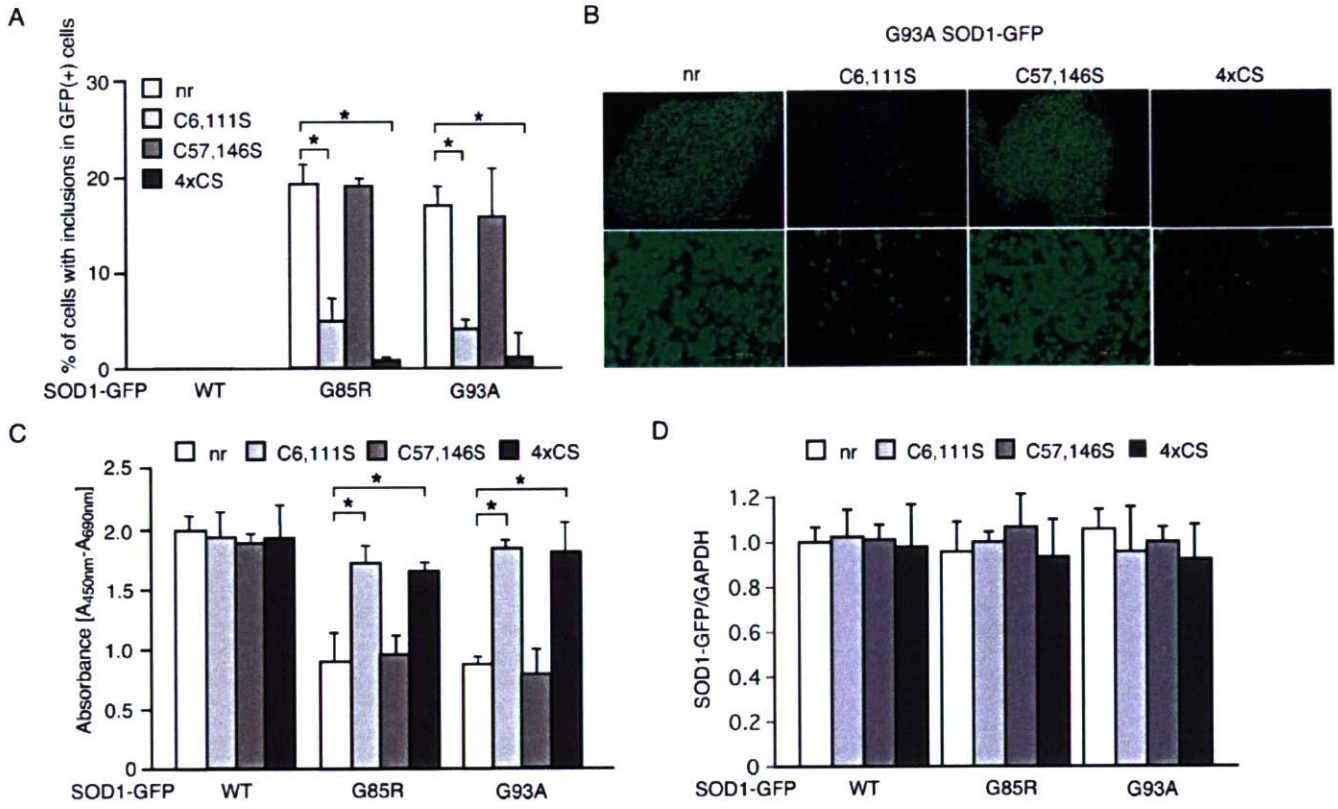

FIGURE 4. **Formation of disulfide-linked species of mutant SOD1 strongly correlates with visible aggregate formation and neurotoxicity.** *A*, the frequency of inclusion-bearing cells transfected with wild-type (*WT*), G85R, and G93A mutant SOD1-GFP and their Cys to Ser derivatives. *B*, G93A mutant SOD1-GFP inclusion bodies in 80 × *g* pellet. *Lower panels* are a high magnification image of the portion on the *upper panels* showing the whole pellet. The *scale bar* is equivalent to 10 mm in the *upper panels*, and 200 μm in the *lower panels*. *C*, change in the neurotoxic effect of mutant SOD1-GFP by Cys replacements to Ser. Cell viability was measured by the WST-1-based assay. *D*, all the constructs have equal expression. Transcription levels of SOD1-GFP in Neuro-2a cells expressing WT, G85R, and G93A mutant SOD1 and their Cys to Ser derivatives were examined by quantitative reverse transcription-PCR. Data were normalized with glyceraldehyde-3-phosphate dehydrogenase expression and then represent relative expression levels compared with levels in cells expressing WT SOD1-GFP. Data are mean ± S.D. values of triplicate assays. Statistical analyses were carried out by analysis of variance. *, $p < 0.01$. *nr*, SOD1 without replacing cysteine residues; *4×CS*, all four cysteines replaced by serines.

species are implicated as the aggregation-prone and neurotoxic intermediate of mutant SOD1 *in vivo*.

Effects of Cys^6- and Cys^{111}-mediated Disulfide Linking on the Rate of Mutant SOD1 Degradation—To determine whether replacement of Cys residues affects the degradation of SOD1 proteins, we examined the stability of mutant SOD1 proteins expressed in Neuro-2a cells (Fig. 6, *A* and *B*). Chase experiments with cycloheximide, which halts all cellular protein synthesis, demonstrated that replacement of Cys residues did not influence the stability of wild-type SOD1 protein (Fig. 6*A*). By contrast, although mutant SOD1 showed the enhanced degradation compared with wild-type proteins previously described (18–20), when both Cys^6 and Cys^{111} were replaced with Ser, the degradation of mutant SOD1 was markedly increased (Fig. 6*B*). Replacement of Cys^{57} and Cys^{146} did not significantly change the rate of degradation compared with Cys-native mutant SOD1 protein.

Ubiquityl Ligase Dorfin Ubiquitylates and Promotes Degradation of Disulfide-linked Mutant SOD1—We have previously shown that Dorfin physically binds and ubiquitylates various familial ALS-linked SOD1 mutants and enhances their degradation (20). Thus, we examined whether Cys residues on SOD1 affect the binding and ubiquitylating activities of Dorfin. To this end, Dorfin was co-expressed with wild-type or mutant SOD1 in Neuro-2a cells. Dorfin co-immunoprecipitated with G85R and G93A mutant SOD1s and their Cys^{57}- and Cys^{146}-replaced derivatives (Fig. 7*A*). However, Dorfin interacted with Cys^6- and Cys^{111}-replaced mutant SOD1 only very weakly and failed to bind to mutant SOD1 when all four Cys residues were replaced (Fig. 7*A*). Dorfin did not bind at all to wild-type SOD1. Using an *in vivo* ubiquitylation assay, we further examined whether co-expressed Dorfin enhances the ubiquitylation of Cys-substituted mutant SOD1 (Fig. 7*B*). When Cys-native or Cys^{57}- and Cys^{146}-replaced mutant SOD1s were co-expressed with Dorfin, ubiquitylation of mutant SOD1s were increased; however, co-expression of Dorfin with mutant SOD1 in which Cys^6 and Cys^{111} or all four Cys residues were replaced did not promote ubiquitylation of these mutant SOD1s (Fig. 7*B*). Chase experiments with cycloheximide in the presence or absence of Dorfin demonstrated that degradation of Cys-native and Cys^{57}- and Cys^{146}-replaced mutant SOD1^{G93A} was greatly accelerated when Dorfin was overexpressed, whereas the stability of Cys^6 and Cys^{111} or all four Cys-replaced mutant SOD1G93A were unaffected (Fig. 7*C*). We have previously shown that Dorfin exerts neuroprotective effects by promoting degradation of mutant SOD1 through its ubiquityl ligase activities (20). Co-expression of Dorfin improved the viability of Neuro-2a cells expressing Cys-

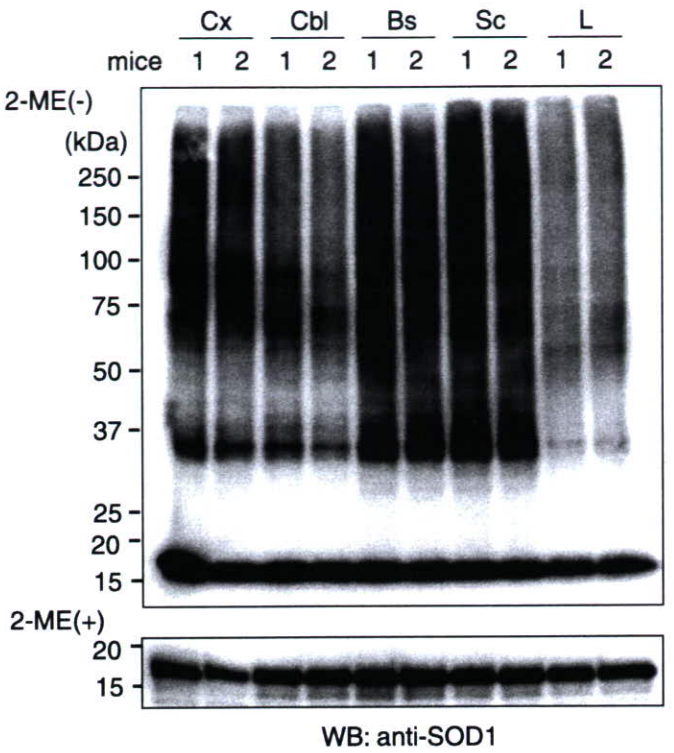

FIGURE 5. **Preferential occurrence of disulfide-cross-linked mutant SOD1 in the affected lesion of ALS model mice.** Western blotting of tissue samples from two 17-week-old symptomatic G93A mutant SOD1-transgenic mice under non-reducing (*upper panel*) and reducing (*lower panel*) conditions. *Cx*, cerebral cortex; *Cbl*, cerebellum; *Bs*, brain stem; *Sc*, spinal cord; *L*, liver.

native and Cys^{57}- and Cys^{146}-replaced mutant $SOD1^{G93A}$ (Fig. 7*D*).

DISCUSSION

Mutations in the *SOD1* gene cause familial ALS through the gain of a toxic function, however, the nature of this toxic function remains largely unknown (31). Ubiquitylated aggregates of mutant SOD1 proteins in affected lesions are a pathological hallmark of the disease (32) and suggest their relation to neurotoxicity. Recent biochemical studies suggest that the immature disulfide-reduced forms of the familial ALS mutant SOD1 proteins play a critical role in this neurotoxicity; *in vitro*, these forms tend to misfold, oligomerize, and readily undergo incorrect disulfide bond formation upon mild oxidative stress (16, 33). Among the more than 100 ALS-associated human SOD1 mutants, some cannot intrinsically form the essential intramolecular disulfide bonds. One of the conserved Cys residues, Cys^{146}, is missing in some of the mutants, such as the Leu^{126} del TT (stop at 131) and Gly^{127} ins TGGG (stop at 133); however, it has been reported that minute quantities of SOD1 aggregates can cause the disease in mice expressing the truncated mutant, Gly^{127} ins TGGG (stop at 133) (34). Furthermore, a significant fraction of the insoluble SOD1 aggregates in the spinal cord of ALS model mice contain multimers cross-linked via intermolecular disulfide bonds (17, 35). In the present study, we showed that non-physiological intermolecular disulfide bonds involving Cys^{6} and Cys^{111} of the mutant SOD1 were important for high molecular weight aggregate formation, ubiquitylation, and neurotoxicity *in vivo*, all of which were dramatically reduced in Neuro-2a cells when these residues were replaced with serines.

Human SOD1 has two free cysteine residues, Cys^{6} and Cys^{111} (36). Cys^{6} is located adjacent to the dimer interface pointed toward the interior of the β-barrel and is solute-inaccessible in the native, folded conformation. Cys^{111} is located near the surface and is solute-accessible and -reactive, often becoming blocked during purification (37). Replacement of the free Cys residues increased the resistance to thermal inactivation (38). Increased resistance of mutant SOD1s is due to increased resistance to irreversible unfolding and relatively unaffected by changes in conformational stability (39). Our data, showing that aggregate formation of mutant SOD1 is reduced when Cys^{6} and Cys^{111} are replaced with serines, are compatible with these observations. Mutations of the Cys^{6} residue (C6F and C6G) still result in familial ALS (4), and in a transgenic mouse expressing mouse SOD1 retaining cystines 6, 57, and 146 but lacking

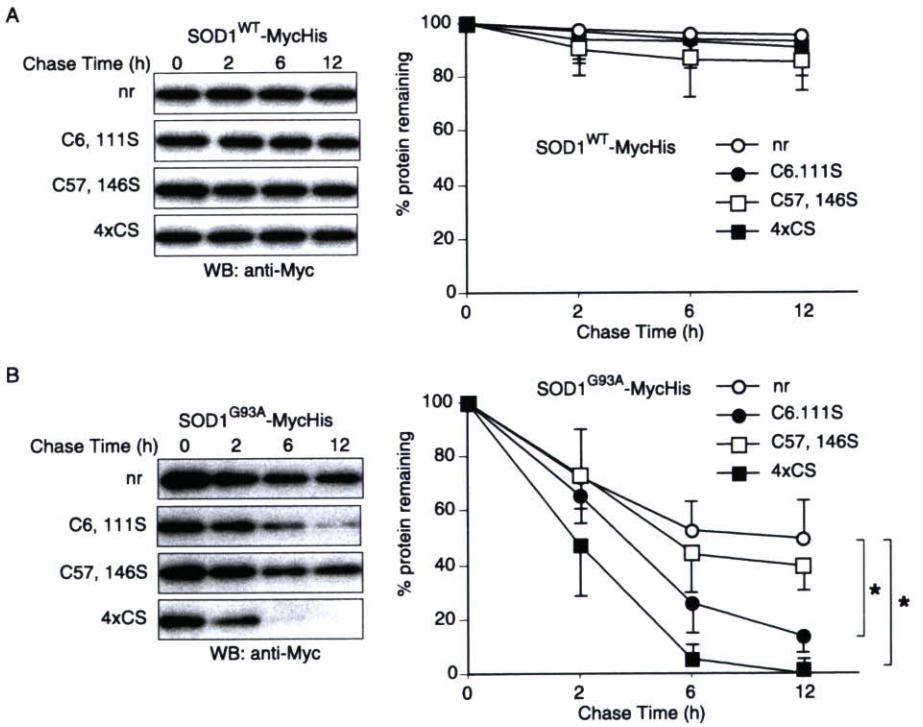

FIGURE 6. **Effects of disulfide-linking at Cys^{6} and Cys^{111} on the rate of mutant SOD1 degradation.** Cycloheximide chase analysis on Neuro-2a cells expressing (*A*) wild-type (*WT*) and (*B*) G93A mutant SOD1 and their Cys to Ser derivatives. Western blots showing levels of SOD1 protein at various times after the cycloheximide chase are in the *left panels*. Quantitative data on the right are mean ± S.D. values of three independent experiments. Statistical analyses were carried out by analysis of variance. *, $p < 0.01$. *nr*, SOD1 without cysteine residue replacement; *4×CS*, all four cysteines replaced by serines.

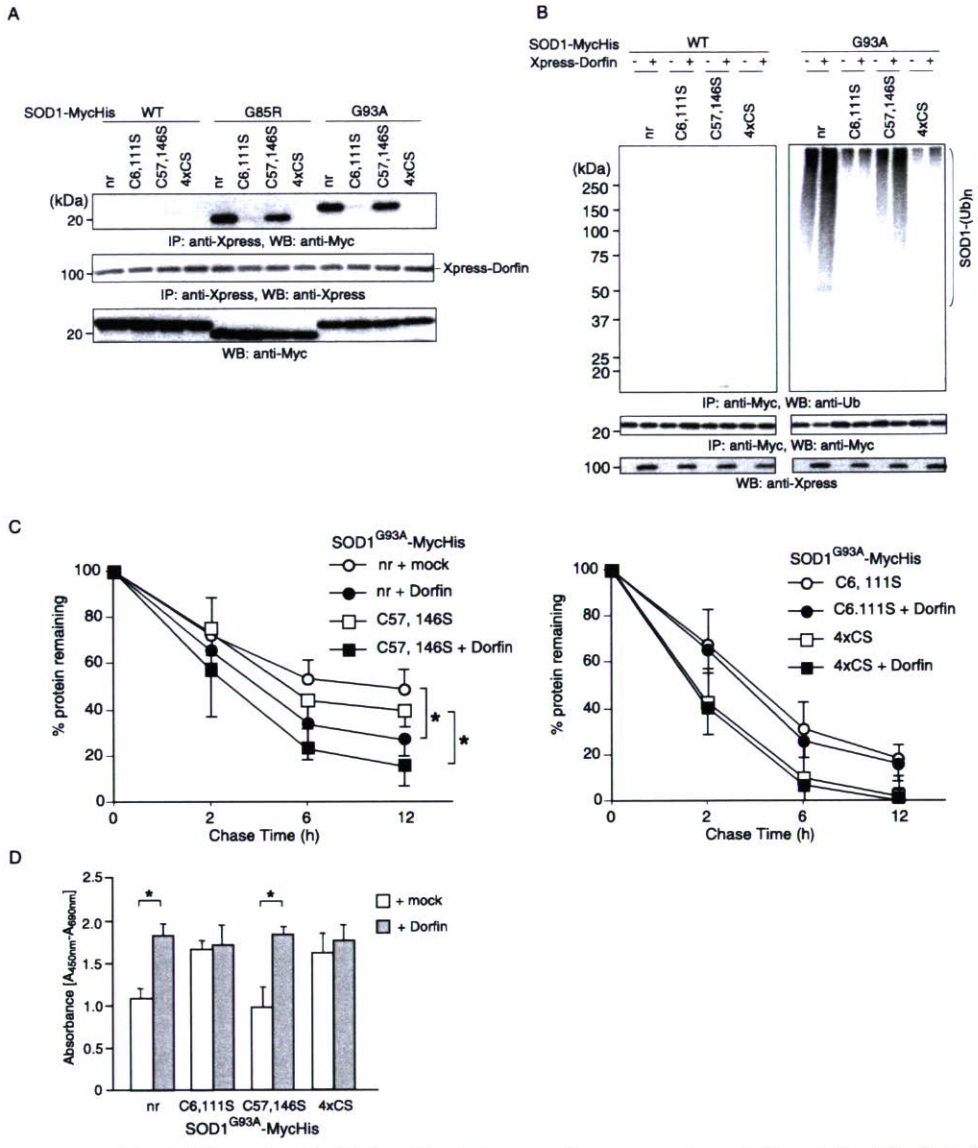

FIGURE 7. **Ubiquityl ligase Dorfin binds, ubiquitylates, and promotes degradation of disulfide-linked mutant SOD1.** *A*, replacement of Cys^6 and Cys^{111} nearly eliminated the interaction of Dorfin with mutant SOD1. Various SOD1-MycHis were co-transfected with Xpress-Dorfin. After immunoprecipitation with anti-Xpress antibody, the resulting precipitates and cell lysates were analyzed by Western blotting with anti-Myc antibody. *B, in vivo*, Dorfin failed to promote ubiquitylation of mutant SOD1 with the Cys^6 and Cys^{111} replacement. Western blotting of SOD1-Myc-His immunoprecipitates with anti-ubiquitin antibody. *C*, Dorfin failed to promote degradation of mutant SOD1 with both Cys^6 and Cys^{111} replaced. Cycloheximide chase analysis of G93A mutant SOD1 with Cys^6 and Cys^{111}-replacements (*left panel*) or with Cys^{57} and Cys^{146}-replacements (*right panel*) in the presence or absence of overexpressed Xpress-Dorfin. *D*, Dorfin prevented neurotoxicity by mutant SOD1 with intact Cys^6 and Cys^{111} residues. Cell viability was measured by the WST-1-based assay. Data are mean ± S.D. values of three independent experiments. Statistical analyses were carried out by unpaired *t* test. *, $p < 0.01$. *nr*, SOD1 without replacement in cysteine residue; *4×CS*, all four cysteines replaced by serines.

111 and with a G86R mutation corresponding to G85R mutation in human SOD1, degeneration of motor neurons in the spinal cord has been observed (40). These results imply that, if one of either the Cys^6 or Cys^{111} residues is present, it can still be a disease-causing SOD1. Our data here also revealed that replacement of only one of the Cys residues at positions 6 or 111 had modest effects on the formation of aggregates (Fig. 2).

Cytoplasmic proteins are degraded mainly via two pathways, the ubiquitin-proteasome pathway (6) and via autophagy (7). Previous studies have shown that mutant SOD1 proteins are turned over more rapidly than wild-type SOD1 (12, 18, 19). Two distinct ubiquitin ligases, Dorfin and NEDL1, were reported to specifically ubiquitylate mutant but not wild-type SOD1 (20, 21). These studies suggest that mutant SOD1 is degraded by the ubiquitin-proteasome pathway and that the accelerated turnover of mutant SOD1 is mediated in part by this pathway. Impairment of the proteasome activities may contribute to ALS pathogenesis (28, 41, 42). We showed here that proteasome inhibition led to a dose-dependent accumulation of aberrant disulfide-linked high molecular weight mutant SOD1 (Fig. 1), suggesting that disulfide-linking mediates ubiquitylation of mutant SOD1. In fact, we found that Dorfin ubiquitylated mutant SOD1 by recognizing the Cys^6 and Cys^{111} disulfide cross-linked form and targeted it for proteasomal degradation (Fig. 7). Mutant SOD1, in which the Cys^6 and Cys^{111} were replaced, was not ubiquitylated (Fig. 3), and its rate of degradation was not affected in the presence of Dorfin (Fig. 7). It is possible that mutant SOD1 lacking Cys^6 and Cys^{111} may be degraded directly by the proteasome without ubiquitylation (43) or by autophagy (44), but further studies are needed to address this issue.

The appearance of mutant SOD1 aggregates in motor neurons of familial ALS patients and mouse models has suggested that aggregation plays an important role in neurotoxicity (31). However, conflicting results have been reported on the correlation between aggregate formation and cell death. One report showed that aggregate formation of mutant $SOD1^{A4V}$ and $SOD1^{V148G}$ does not correlate with cell death (45), whereas another study using live cell-imaging techniques reported that the ability of mutant $SOD1^{G85R}$ and $SOD1^{G93A}$ proteins to form aggregates directly correlates with neuronal cell death (46). These controversies also exist in other neurodegenerative diseases (47, 48). In this study, we clearly showed a direct link among intermolecular disulfide bond-mediated high molecular weight complex formation, visible aggregate formation, and neurotoxicity (Figs. 2–4).

Furukawa *et al.* (16) reported that formation of disulfide-linked multimers need not involve the non-conserved Cys residues, Cys^6 and Cys^{111}, and that the conserved Cys residues, Cys^{57} and Cys^{146}, play an important role in the apo-form of

SOD1 multimerization upon oxidative stress. Our results underscore the importance of Cys^{6} and Cys^{111} for high molecular weight aggregate formation, ubiquitylation, and neurotoxicity in Neuro-2a cells. This discrepancy may result from differences in experimental conditions; we studied human SOD1 proteins expressed in Neuro-2a cells, and Furukawa *et al.* used the purified apo-form of human SOD1 from *Escherichia coli.* Further studies will clarify the roles of each of the Cys residues of the mutant SOD1 protein in the ALS pathogenesis *in vivo* by generating transgenic mice bearing mutant SOD1 lacking Cys^{6} and Cys^{111} or Cys^{57} and Cys^{146}.

REFERENCES

1. McCord, J. M., and Fridovich, I. (1969) *J. Biol. Chem.* **244,** 6049–6055
2. Fridovich, I. (1974) *Adv. Enzymol. Relat. Areas. Mol. Biol.* **41,** 35–97
3. Rosen, D. R. (1993) *Nature* **364,** 362
4. Valentine, J. S., Doucette, P. A., and Potter, S. Z. (2005) *Annu. Rev. Biochem.* **74,** 563–593
5. Crapo, J. D., Oury, T., Rabouille, C., Slot, J. W., and Chang, L. Y. (1992) *Proc. Natl. Acad. Sci. U. S. A.* **89,** 10405–10409
6. Fridovich, I. (1986) *Adv. Enzymol. Relat. Areas. Mol. Biol.* **58,** 61–97
7. Fisher, C. L., Cabelli, D. E., Tainer, J. A., Hallewell, R. A., and Getzoff, E. D. (1994) *Proteins* **19,** 24–34
8. Arnesano, F., Banci, L., Bertini, I., Martinelli, M., Furukawa, Y., and O'Halloran, T. V. (2004) *J. Biol. Chem.* **279,** 47998–48003
9. Freedman, R. B. (1995) *Curr. Opin. Struct. Biol.* **5,** 85–91
10. Lindenau, J., Noack, H., Possel, H., Asayama, K., and Wolf, G. (2000) *Glia* **29,** 25–34
11. Tiwari, A., and Hayward, L. J. (2003) *J. Biol. Chem.* **278,** 5984–5992
12. Borchelt, D. R., Lee, M. K., Slunt, H. S., Guarnieri, M., Xu, Z. S., Wong, P. C., Brown, R. H., Jr., Price, D. L., Sisodia, S. S., and Cleveland, D. W. (1994) *Proc. Natl. Acad. Sci. U. S. A.* **91,** 8292–8296
13. Ratovitski, T., Corson, L. B., Strain, J., Wong, P., Cleveland, D. W., Culotta, V. C., and Borchelt, D. R. (1999) *Hum. Mol. Genet* **8,** 1451–1460
14. Rakhit, R., Crow, J. P., Lepock, J. R., Kondejewski, L. H., Cashman, N. R., and Chakrabartty, A. (2004) *J. Biol. Chem.* **279,** 15499–15504
15. Doucette, P. A., Whitson, L. J., Cao, X., Schirf, V., Demeler, B., Valentine, J. S., Hansen, J. C., and Hart, P. J. (2004) *J. Biol. Chem.* **279,** 54558–54566
16. Furukawa, Y., and O'Halloran, T. V. (2005) *J. Biol. Chem.* **280,** 17266–17274
17. Furukawa, Y., Fu, R., Deng, H. X., Siddique, T., and O'Halloran, T. V. (2006) *Proc. Natl. Acad. Sci. U. S. A.* **103,** 7148–7153
18. Hoffman, E. K., Wilcox, H. M., Scott, R. W., and Siman, R. (1996) *J. Neurol. Sci.* **139,** 15–20
19. Johnston, J. A., Dalton, M. J., Gurney, M. E., and Kopito, R. R. (2000) *Proc. Natl. Acad. Sci. U. S. A.* **97,** 12571–12576
20. Niwa, J., Ishigaki, S., Hishikawa, N., Yamamoto, M., Doyu, M., Murata, S., Tanaka, K., Taniguchi, N., and Sobue, G. (2002) *J. Biol. Chem.* **277,** 36793–36798
21. Miyazaki, K., Fujita, T., Ozaki, T., Kato, C., Kurose, Y., Sakamoto, M., Kato, S., Goto, T., Itoyama, Y., Aoki, M., and Nakagawara, A. (2004) *J. Biol. Chem.* **279,** 11327–11335
22. Niwa, J., Ishigaki, S., Doyu, M., Suzuki, T., Tanaka, K., and Sobue, G. (2001) *Biochem. Biophys. Res. Commun.* **281,** 706–713
23. Marin, I., and Ferrus, A. (2002) *Mol. Biol. Evol.* **19,** 2039–2050
24. Lee, H. J., and Lee, S. J. (2002) *J. Biol. Chem.* **277,** 48976–48983
25. Scherzinger, E., Lurz, R., Turmaine, M., Mangiarini, L., Hollenbach, B., Hasenbank, R., Bates, G. P., Davies, S. W., Lehrach, H., and Wanker, E. E. (1997) *Cell* **90,** 549–558
26. Bailey, C. K., Andriola, I. F., Kampinga, H. H., and Merry, D. E. (2002) *Hum. Mol. Genet.* **11,** 515–523
27. Wang, J., Xu, G., and Borchelt, D. R. (2002) *Neurobiol. Dis.* **9,** 139–148
28. Urushitani, M., Kurisu, J., Tsukita, K., and Takahashi, R. (2002) *J. Neurochem.* **83,** 1030–1042
29. Gurney, M. E., Pu, H., Chiu, A. Y., Dal Canto, M. C., Polchow, C. Y., Alexander, D. D., Caliendo, J., Hentati, A., Kwon, Y. W., Deng, H. X., Chen, W., Zhai, P., Sufit, R. L., and Siddique, T. (1994) *Science* **264,** 1772–1775
30. Bruijn, L. I., Houseweart, M. K., Kato, S., Anderson, K. L., Anderson, S. D., Ohama, E., Reaume, A. G., Scott, R. W., and Cleveland, D. W. (1998) *Science* **281,** 1851–1854
31. Cleveland, D. W., and Rothstein, J. D. (2001) *Nat. Rev. Neurosci.* **2,** 806–819
32. Watanabe, M., Dykes-Hoberg, M., Culotta, V. C., Price, D. L., Wong, P. C., and Rothstein, J. D. (2001) *Neurobiol. Dis.* **8,** 933–941
33. Wang, J., Xu, G., and Borchelt, D. R. (2006) *J. Neurochem.* **96,** 1277–1288
34. Jonsson, P. A., Graffmo, K. S., Andersen, P. M., Brannstrom, T., Lindberg, M., Oliveberg, M., and Marklund, S. L. (2006) *Brain* **129,** 451–464
35. Deng, H. X., Shi, Y., Furukawa, Y., Zhai, H., Fu, R., Liu, E., Gorrie, G. H., Khan, M. S., Hung, W. Y., Bigio, E. H., Lukas, T., Dal Canto, M. C., O'Halloran, T. V., and Siddique, T. (2006) *Proc. Natl. Acad. Sci. U. S. A.* **103,** 7142–7147
36. Getzoff, E. D., Tainer, J. A., Stempien, M. M., Bell, G. I., and Hallewell, R. A. (1989) *Proteins* **5,** 322–336
37. Briggs, R. G., and Fee, J. A. (1978) *Biochim. Biophys. Acta* **537,** 86–99
38. McRee, D. E., Redford, S. M., Getzoff, E. D., Lepock, J. R., Hallewell, R. A., and Tainer, J. A. (1990) *J. Biol. Chem.* **265,** 14234–14241
39. Lepock, J. R., Frey, H. E., and Hallewell, R. A. (1990) *J. Biol. Chem.* **265,** 21612–21618
40. Ripps, M. E., Huntley, G. W., Hof, P. R., Morrison, J. H., and Gordon, J. W. (1995) *Proc. Natl. Acad. Sci. U. S. A.* **92,** 689–693
41. Kabashi, E., Agar, J. N., Taylor, D. M., Minotti, S., and Durham, H. D. (2004) *J. Neurochem.* **89,** 1325–1335
42. Cheroni, C., Peviani, M., Cascio, P., Debiasi, S., Monti, C., and Bendotti, C. (2005) *Neurobiol. Dis.* **18,** 509–522
43. Di Noto, L., Whitson, L. J., Cao, X., Hart, P. J., and Levine, R. L. (2005) *J. Biol. Chem.* **280,** 39907–39913
44. Kabuta, T., Suzuki, Y., and Wada, K. (2006) *J. Biol. Chem.* **281,** 30524–30533
45. Lee, J. P., Gerin, C., Bindokas, V. P., Miller, R., Ghadge, G., and Roos, R. P. (2002) *J. Neurochem.* **82,** 1229–1238
46. Matsumoto, G., Stojanovic, A., Holmberg, C. I., Kim, S., and Morimoto, R. I. (2005) *J. Cell Biol.* **171,** 75–85
47. Arrasate, M., Mitra, S., Schweitzer, E. S., Segal, M. R., and Finkbeiner, S. (2004) *Nature* **431,** 805–810
48. Saudou, F., Finkbeiner, S., Devys, D., and Greenberg, M. E. (1998) *Cell* **95,** 55–66

J Neuropathol Exp Neurol

Vol. 66, No. 7
July 2007
pp. 617–627

ORIGINAL ARTICLE

Gene Expressions Specifically Detected in Motor Neurons (Dynactin 1, Early Growth Response 3, Acetyl-CoA Transporter, Death Receptor 5, and Cyclin C) Differentially Correlate to Pathologic Markers in Sporadic Amyotrophic Lateral Sclerosis

Yue-Mei Jiang, PhD, Masahiko Yamamoto, MD, Fumiaki Tanaka, MD, Shinsuke Ishigaki, MD, Masahisa Katsuno, MD, Hiroaki Adachi, MD, Jun-ichi Niwa, MD, Manabu Doyu, MD, Mari Yoshida, MD, Yoshio Hashizume, MD, and Gen Sobue, MD

Abstract

In a differential gene expression profile, we showed previously that dynactin 1 (*DCTN1*), early growth response 3 (*EGR3*), acetyl-CoA transporter (*ACATN*), death receptor 5 (*DR5*), and cyclin C (*CCNC*) were prominently up- or downregulated in motor neurons of sporadic amyotrophic lateral sclerosis (ALS). In the present study, we examined the correlation between the expression levels of these genes and the levels of pathologic markers for motor neuron degeneration (i.e. cytoplasmic accumulation of phosphorylated neurofilament H [pNF-H] and ubiquitylated protein) and the numbers of residual motor neurons in 20 autopsies of patients with sporadic ALS. *DCTN1* and *EGR3* were widely downregulated, and the changes in gene expression were correlated to the number of residual motor neurons. In particular, *DCTN1* was markedly downregulated in most residual motor neurons before the accumulation of pNF-H, even in cases with well-preserved motor neuron populations. *ACATN*, *DR5*, and *CCNC* were upregulated in subpopulations of residual motor neurons, and their expression levels were well correlated with the levels of pNF-H accumulation and the number of residual motor neurons. The expressions of *DCTN1*, *EGR3*, *ACATN*, and *DR5* were all markedly altered before ubiquitylated protein accumulation. *DCTN1* downregulation appears to be an early event before the appearance of neurodegeneration markers, whereas upregulations of *DR5* and *CCNC* are relatively later phenomena associated with pathologic markers and leading to neuronal death. The sequence of motor neuron-specific gene expression changes in sporadic ALS can be beneficial information in developing appropriate therapeutic strategies for neurodegeneration.

Key Words: Amyotrophic lateral sclerosis (ALS), Axonal transport, Cell death, Dynactin 1, Motor neuron.

INTRODUCTION

Amyotrophic lateral sclerosis (ALS) is a devastating neurodegenerative disease characterized by loss of motor neurons in the spinal cord, brainstem, and motor cortex (1), causing weakness of the limbs, abnormalities of speech, and difficulties in swallowing. The weakness ultimately progresses to respiratory impairment and half of the patients die within 3 years of the onset of symptoms, largely due to respiratory failure. About 5% to 10% of all patients with ALS show familial traits, and 20% to 30% of patients with familial ALS have a mutation in the copper/zinc superoxide dismutase 1 gene (*SOD1*). However, in more than 90% of patients with ALS, the disease is sporadic and does not show any familial traits. The presence of Bunina bodies in the remaining spinal motor neurons is a hallmark of cases of sporadic ALS (2, 3). There is at present no obvious consensus understanding of the pathogenic mechanism or an effective therapeutic approach for sporadic ALS, although several hypotheses, including oxidative stress, glutamate excitotoxicity, impaired axonal transport, neurofilament disintegration, mitochondrial dysfunction, neurotrophic deprivation, and proteasomal dysfunction have been proposed as causal mechanisms of motor neuron degeneration (4–11). In contrast, wide-ranging research activities have been initiated for a subgroup of patients with familial ALS, those with mutant *SOD1*, including a search for the pathogenic mechanisms of mutant SOD1-induced motor neuron death and the examination of therapeutic perspectives using a transgenic rodent model for mutant SOD1 familial ALS (12–14).

One effective approach to begin the uncovering of the pathogenic mechanism of sporadic ALS is a description of

From the Department of Neurology (Y-MJ, MY, FT, SI, MK, HA, J-IN, MD, GS), Nagoya University Graduate School of Medicine, Nagoya, Japan; Department of Speech Pathology and Audiology (MY), Aichi Gaguin University School of Health Science, Nisshin, Aichi, Japan; and Department of Neuropathology (MY, YH), Institute for Medical Science of Aging, Aichi Medical University School of Medicine, Nagakute, Aichi, Japan.

Drs. Jiang and Yamamoto contributed equally to this work.

Send correspondence and reprint requests to: Dr. Gen Sobue, Department of Neurology, Nagoya University Graduate School of Medicine, Nagoya 466-8550, Japan; E-mail: sobueg@med.nagoya-u.ac.jp

This work was supported by the 21st Century COE Program "Integrated Molecular Medicine for Neuronal and Neoplastic Disorders" from the Ministry of Education, Culture, Sports, Science and Technology of Japan, and grants from the Ministry of Health, Labor and Welfare of Japan.

the gene expression profile of motor neurons. Motor neuron-specific gene expression profiling would eventually lead us to a profound understanding of the pathophysiology of motor neuron degeneration in sporadic ALS. We have successfully created such a motor neuron-specific gene expression profile in patients with sporadic ALS by using microarray technology combined with laser-captured microdissection, the results of which were further verified by in situ hybridization and quantitative wide-ranging research activities (15). The genes with differential expressions in these profiles were particularly related to axonal transport, transcription, energy production, cell death, and protection from cell death. Gene expressions of dynactin 1 (*DCTN1*) and early growth response 3 (*EGR3*), related to cytoskeleton/axonal transport and transcription, respectively, were markedly decreased in motor neurons, whereas cell death-associated genes such as death receptor 5 (*DR5*), cyclin C (*CCNC*), and acetyl-CoA transporter (*ACATN*) were greatly upregulated. It is, however, uncertain how these gene expression alterations correlate with motor neuron degeneration and death and whether they play a role in the pathogenesis of sporadic ALS. A description of the molecular events underlying motor neuron degeneration in sporadic ALS, even particular short aspects of a long sequence of the degeneration process, would provide a beneficial therapeutic avenue for sporadic ALS by enabling development of a disease model simulating these molecular events.

In this study we further characterized the gene expression profiles of *DCTN1*, *EGR3*, *ACATN*, *DR5*, and *CCNC* in individual motor neurons and compared their expression levels with those of known motor neuron neurodegeneration markers, cytoplasmic accumulations of phosphorylated neurofilament H (pNF-H), ubiquitylated proteins, and with neuronal loss (5, 16–18). We found that changes in expression levels of these genes differentially reflect the motor neuron degeneration process, and, in particular, *DCTN1* is extensively downregulated before the appearance of these degeneration markers.

MATERIALS AND METHODS

Tissues From Patients with Amyotrophic Lateral Sclerosis and Control Patients

Specimens of lumbar spinal cord (L4–L5 segments) from 20 patients with sporadic ALS (11 male and 9 female) and 8 neurologically normal patients (4 male and 4 female) as controls were obtained at autopsy. The diagnosis of ALS was confirmed by El Escorial diagnostic criteria defined by the World Federation of Neurology and by histopathologic findings, particularly the presence of Bunina bodies (2, 3). All patients with ALS had sporadic ALS and showed no hereditary traits. Patients with a *SOD1* mutation were excluded. The collection of tissues and their use for this study were approved by the ethics committee of Nagoya University Graduate School of Medicine. The ages for patients with ALS and control patients were 63.3 ± 11.5 (mean ± SD) (range 43–80) and 65.4 ± 12.7 (42–79) years, respectively, and the ALS illness duration was 2.9 ± 0.87 (1.2–4.3) years. The postmortem intervals to autopsy for patients with ALS and control patients were 7.3 ± 3.9 (3–15) and 8.6 ± 3.2 (4–13) hours, respectively. There were no significant differences in either age or postmortem interval between the ALS and control groups. Among 20 patients, severe bulbar symptoms were seen in 14 cases, severe upper limb wasting in 17 cases, and severe lower limb wasting in 13 cases in the advanced stage. The upper motor neuron signs were seen in 13 patients, whereas others showed predominantly lower motor neuron signs. Most of the patients with ALS developed respiratory dysfunction in various degrees, with eventually resulted in respiratory failure in all patients, which was the cause of death. The cause of death in the control patients was pneumonia, cancer, stroke, or acute heart attack. Tissues were immediately frozen in liquid nitrogen and stored at −80°C until use. Parts of the lumbar spinal cord were fixed in 10% buffered formalin solution and processed for paraffin sections. The sections were stained with hematoxylin and eosin and Klüver-Barrera techniques and further histologic assessments were performed.

Selection of Genes Examined Based on Our Previous Microarray Analysis in Laser-Captured Motor Neurons of Patients with Sporadic Amyotrophic Lateral Sclerosis

By using microarray technology combined with laser-captured microdissection, gene expression profiles of degenerating spinal motor neurons isolated from autopsied patients with sporadic ALS were previously reported (15). Three percent of genes examined were downregulated, and 1% were upregulated. We selected 5 genes (*DCTN1* associated with cytoskeleton/axonal transport *EGR3* as a transcription factor, and *ACATN*, *DR5* and *CCNC* as cell death-associated genes), which were most prominently down- or upregulated (15). These changes in gene expression were confirmed by cluster analyses of hierarchical clustering, self-organizing maps, and principal component analyses after logarithmic transformation, as motor neuron-specific gene expression changes distinctive from the spinal ventral horn as a whole, and their alterations were further quantitatively verified by real-time wide-ranging research activities and in situ hybridization. In addition, these 5 genes were chosen for the present study because they cover a wide range and represent different aspects of the functional hierarchy.

In Situ Hybridization

Frozen, 10-μm-thick spinal cord sections were prepared and immediately fixed in 4% paraformaldehyde. The sections were then treated with 0.1% diethylpyrocarbonate twice for 15 minutes and prehybridized at 45°C for 1 hour. Digoxigenin-labeled cRNA probes were generated from linearized plasmids for the genes of interest using SP6 or T7 polymerase (Roche Diagnostics, Basel, Switzerland). Gene names, GenBank accession numbers, probe positions (nucleotide [nt] number), and probe sizes (base pairs [bp]) were as follows: acetyl-CoA transporter (*ACATN*), D88152, nt 397–741, 345 bp; dynactin 1 (*DCTN1*), NM_004082, nt 2392–2774, 383 bp; death receptor 5 (*DR5*), NM_004082, nt 682–1070, 389 bp; and early growth response 3 (*EGR3*), NM_004430, nt 1433–1794, 362 bp. After prehybridization

the sections were hybridized with digoxigenin-labeled cRNA probes overnight at 45°C. The washed sections were incubated with alkaline phosphatase-conjugated, anti-digoxigenin antibody (Roche Diagnostics). The signal was visualized with nitro blue tetrazolium/5-bromo-4-chloro-3-indolyl phosphate (Roche Diagnostics). No hybridization signal was observed with the sense probe for the expression of each gene in spinal motor neurons.

Immunohistochemistry

Frozen, 10-μm-thick spinal cord sections were prepared and immediately fixed in 4% paraformaldehyde. The sections were then blocked with 2% bovine serum albumin (Sigma) in Tris-buffered saline at room temperature for 20 minutes and incubated with either a monoclonal antibody against the phosphorylated epitope in the tail domain of neurofilament H (anti-SMI 31, 1:1000; Sternberger Monoclonals Inc., Lutherville, MD), anti-cyclin C antibody (1:200; Santa Cruz Biotechnology, Santa Cruz, CA), or anti-ubiquitin (1:1000; Santa Cruz Biotechnology) overnight at 4°C. Subsequent procedures were carried out using the EnVision+Kit/HRP (DAB) (DAKO, Glostrup, Denmark) according to the manufacturer's protocol.

Quantitative Assessment of Gene Expression Levels, Population of Residual Motor Neurons, and Cytoplasmic Accumulation of Phosphorylated Neurofilament H and Ubiquitylated Proteins

To assess gene and protein expression levels in spinal motor neurons, signal intensities of in situ hybridization and immunohistochemistry, respectively, were quantified using a CCD image analyzer (Zeiss Axiovert S100TV) as described previously (19, 20). Images of individual motor neurons on transverse sections of spinal cord with signals for *DCTN1*, *EGR3*, *ACATN*, *DR5*, or CCNC and pNF-H were captured at the desired magnification and stored with image software (Adobe Photoshop). Grey-scale levels in 65,536 gradations of the images were quantitatively analyzed with image analysis software (Image Gauge version 4.0, Fujifilm, Tokyo, Japan). Signal intensities were expressed as individual intracellular cytoplasmic signal levels (arbitrary absorbance units/mm^2) of motor neuron for each gene of interest by subtracting the mean background levels of 3 regions of interest in each section. We also assessed motor neurons harboring ubiquitylated proteins on the anti-ubiquitin-stained sections. Motor neurons with dot-like accumulations, skein-like accumulations, or large inclusions of cytoplasmic ubiquitylated proteins were designated as positive for ubiquitylated protein accumulation.

To count the number of remaining spinal motor neurons, 10-μm-thick serial sections were prepared from the lumber segment of spinal cords and every 10th section was stained with the Klüver-Barrera technique. The ventral spinal horn was designated as the grey matter ventral to the line through the central spinal canal perpendicular to the ventral spinal sulcus, and the residual motor neuron population was defined as the number of relatively large-sized ventral horn cells of 24.8 μm or more in diameter with distinct nucleoli on 10 sections, as described previously (21). Our previous study demonstrated the neuron loss predominantly in the relatively large neurons in ALS (21).

The frequency of motor neurons showing changes in gene expression levels was assessed in at least 10 transverse sections from each of 20 patients with ALS and 8 control patients. The number of motor neurons with gene expression levels more than ±2 SDs from the control levels was expressed as a percentage of motor neurons. Ten to > 100 motor neurons were examined for each individual case.

To investigate the correlation between gene expression levels and pathologic markers in an individual motor neuron we used consecutive transverse spinal cord sections. Ten sets of consecutive sections for each gene of interest were prepared from each patient and the correlations of gene expression levels with pNF-H accumulation levels and positive or negative ubiquitylated protein accumulations were assessed on individual motor neurons. This assessment was performed for 8 representative patients with ALS and 8 control patients whose sections were available for examination.

Statistical Analyses

Simple correlation tests were performed to assess the correlation of gene expression levels of *DCTN1*, *EGR3*, *ACATN*, and *DR5* and protein expression of CCNC, with the degree of pNF-H accumulation in individual motor neurons. This test was also applied to assess the correlation of the gene expression changes with the numbers of residual motor neurons. Mann-Whitney U tests were used to compare gene expression levels among the motor neurons that were either positive or negative for ubiquitylated proteins in patients with ALS and in control patients. Significance levels were set to $p < 0.05$.

RESULTS

Differential Frequencies of Gene Expression Changes in Residual Motor Neurons: *DCTN1* Is Highly Downregulated

Among the genes examined, *DCTN1* and *EGR3* were downregulated in the vast majority of spinal motor neuron populations in most patients (Fig. 1A, B). In 15 of 20 patients, all of the residual motor neurons had reduced *DCTN1* expression compared with controls (Fig. 1B). Ten of the 20 patients showed downregulation of *EGR3* in all residual neurons (Fig. 1B). *ACATN*, by contrast, was upregulated in all residual motor neurons in only 8 of 20 patients (Fig. 1A, B). *DR5* was upregulated in subpopulations of motor neurons, whereas only 4 patients had upregulated gene expression in all of the residual neurons (Fig. 1A, B). Nuclear accumulation of CCNC protein assessed by immunohistochemistry was observed in only a small percentage of motor neurons in most patients (Fig. 1A, B). There were no patients with CCNC nuclear accumulation in all of the residual neurons (Fig. 1B). Cytoplasmic accumulation of pNF-H was seen in more than half of the residual motor neurons in most of the patients (Fig. 1A). Quantitative assessment showed

that in 9 of the 20 patients, all of the residual motor neurons were positive for pNF-H (Fig. 1B). Thus, the frequency of residual motor neurons with gene up- or downregulation was markedly different depending on the individual gene. This gene-dependent differential gene expression among the residual motor neurons is clearly demonstrated in Figure 1C. Two consecutive transverse sections were subjected to in situ hybridization with different gene probes. *DCTN1*

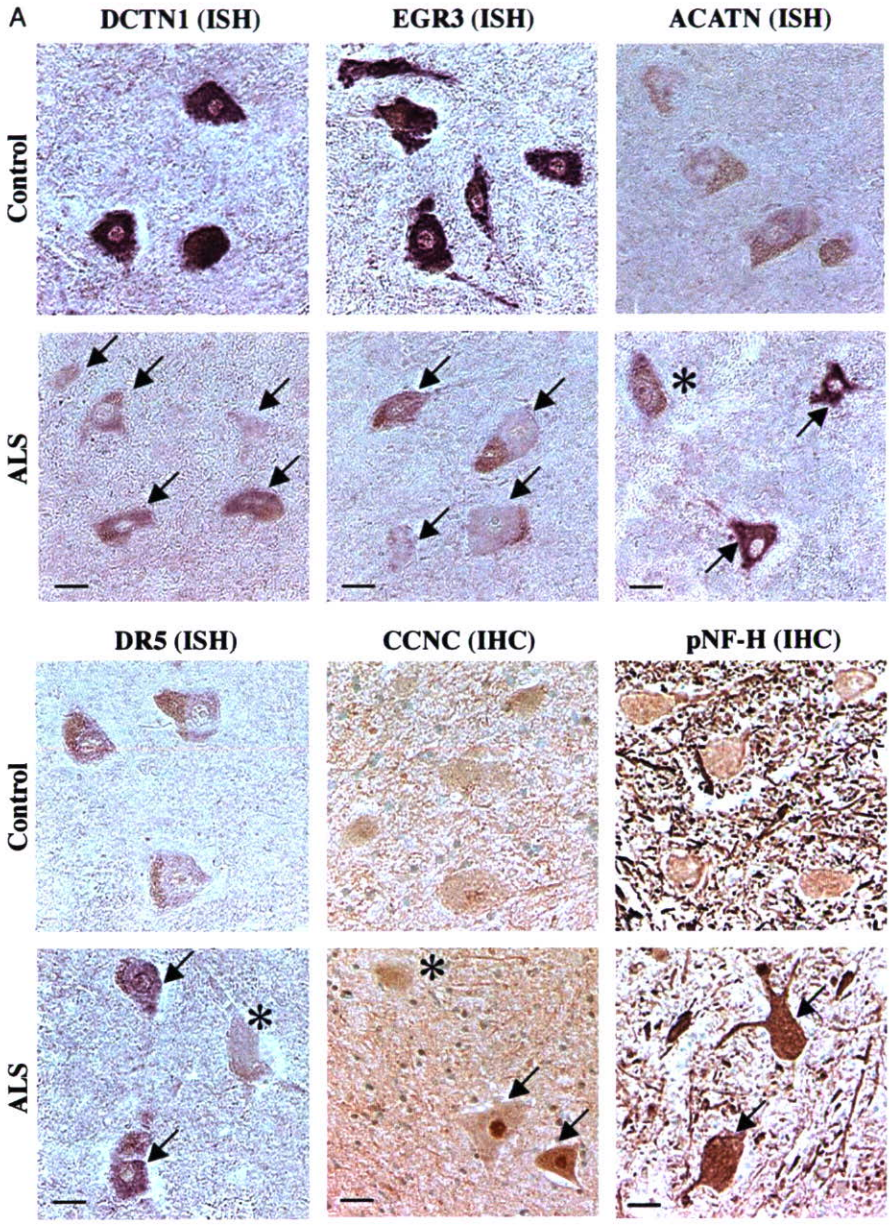

FIGURE 1. In situ hybridization (ISH) and immunohistochemistry (IHC) in spinal motor neurons. **(A)** Representative ISHs are shown for dynactin 1 (*DCTN1*), early growth response 3 (*EGR3*), acetyl-CoA transporter (*ACATN*), and death receptor 5 (*DR5*). The antisense probe detects positive signals for the expression of each gene in spinal motor neurons for patients with amyotrophic lateral sclerosis (ALS) and/or control patients, but the sense probe does not (15). RNase treatment before the hybridization abolished the hybridization signals. IHC was performed for cyclin C (CCNC) and phosphorylated neurofilament H (pNF-H). The nuclear staining of CCNC was prominent in ALS motor neurons. Lipofuscin granules are seen as yellowish granules. **(B)** Percentage of motor neurons with gene expression or protein accumulation changes, relative to control levels, among the residual motor neurons in 20 patients with ALS. The quantitative analyses of gene expression and frequency assessments are described in the Materials and Methods section. **(C)** ISH of 2 genes in consecutive sections demonstrates the relationship between up- and downregulated genes in individual motor neurons. *DCTN1* was downregulated to a great extent in all the remaining motor neurons in ALS, whereas *ACATN* and *DR5* were upregulated in only a subpopulation of motor neurons. Arrows denote motor neurons with gene expression changes, and asterisks denote those without changes compared with controls. Scale bars = 25 μm.

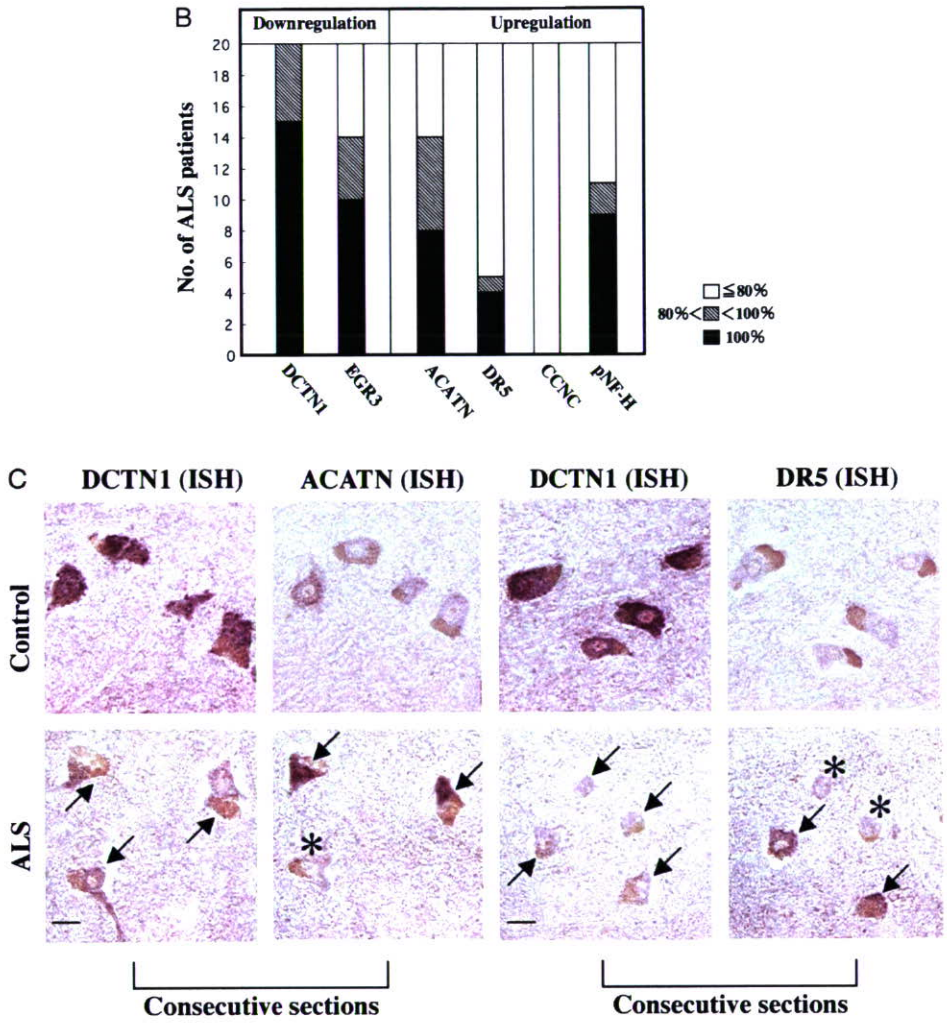

FIGURE 1. (continued)

expression was reduced in all the neurons in each panel, whereas some of the residual motor neurons showed unchanged *ACATN* and *DR5* gene expression (Fig. 1C). Moreover, *DCTN1* expression was preserved in neurons other than motor neurons such as those in the dorsal nucleus of Clarke and the intermediolateral nucleus in spinal cords, Purkinje cells of the cerebellum and cortical neurons in the occipital cortex in patients with ALS as well as control patients (data not shown). These findings indicate that, among the genes examined, downregulation of *DCTN1* was specific and extensive in the spinal motor neurons, whereas cell death-related genes such as *ACATN* and *DR5,* and the protein CCNC were upregulated in only subpopulations of motor neurons.

Gene Expression Changes Are Differentially Correlated With the Population of Residual Motor Neuron: *DCTN1* is Markedly Downregulated Even in Patients With Relatively Well-Preserved Motor Neuron Populations

When the numbers of motor neurons with given gene expression or protein accumulation changes were compared with the numbers of residual motor neurons in the 20 patients, changes in *DR5*, pNF-H, *EGR3*, *ACATN* and *DCTN1* were correlated with the residual motor neuron population ($r = 0.49–0.83$, $p < 0.05$ to 0.0001, Fig. 2). Among them, *DCTN1* expression was most prominently downregulated, even in patients with relatively well-preserved motor neurons, suggesting that *DCTN1* downregulation may be occurring even in early stages of the disease. The changes in expression of *EGR3*, *ACATN*, and *DR5* in patients with well-preserved motor neuron populations were relatively mild compared with that of *DCTN1* (Fig. 2). The change in DR5 expression was less correlated with the residual motor neuron population than that of other genes.

Gene Expression Changes are Differentially Correlated With the Extent of Motoneuronal Cytoplasmic Phosphorylated Neurofilament H Accumulation: *DCTN1* and *EGR3* Are Markedly Downregulated Before Phosphorylated Neurofilament H Accumulation

The correlation of gene expression and pNF-H accumulation, a marker of neuronal degeneration, in individual motor

neurons was assessed on consecutive sections (Fig. 3A, B). *DCTN1* and *EGR3* downregulations were both marked and independent of the degree of cytoplasmic pNF-H accumulation (Fig. 3B), implying that these genes were widely downregulated even in motor neurons with little or no pNF-H accumulation. By contrast, levels of *ACATN*, *DR5*, and CCNC ranged from just above the control levels to much higher levels and were well correlated with the degree of cytoplasmic pNF-H accumulation ($r = 0.48–0.60$, $p < 0.001$ to 0.0001, Fig. 3B).

These observations indicate that downregulation of *DCTN1* and *EGR3* occurs before the appearance of the neurodegeneration marker pNF-H and thus is a relatively early event in the neurodegeneration process. In contrast, the changes in *ACATN* and *DR5* expression were milder than those in *DCTN1* and *EGR3*, but proportional to pNF-H accumulation, suggesting that their upregulation is a relatively late event, occurring after the appearance of the neurodegeneration marker pNF-H.

Gene Expression Changes Occur Before Appearance of Motoneuronal Cytoplasmic Accumulation of Ubiquitylated Proteins: *DCTN1*, *EGR3*, *ACATN* and *DR5* Are Changed Even in the Motor Neurons Without Ubiquitylated Protein Accumulation

The correlation of gene expression with cytoplasmic accumulation of ubiquitylated protein in individual motor neurons was assessed on consecutive sections (Fig. 4A, B). In patients with ALS, *DCTN1* and *EGR3* were markedly downregulated, and *ACATN* and *DR5* were upregulated in motor neurons both with and without cytoplasmic accumulation of ubiquitylated proteins (Fig. 4B). However, the degree of downregulation or upregulation was significantly greater in the motor neurons with ubiquitylated protein accumulation compared with those without (Fig. 4B), suggesting that cytoplasmic accumulation of ubiquitylated proteins may be partially correlated to expression changes of *DCTN1*, *EGR3*, and *ACATN*. However, because the expression of these genes changed markedly even in the motor neurons without ubiquitylated proteins, it would imply that cytoplasmic ubiquitylated protein accumulation is a rather late event in the process of motor neuron degeneration.

We further examined the correlation between these 4 gene expression levels and subgroups of motor neurons with 3 different types of ubiquitylated protein accumulation (i.e. dot-like accumulations, skein-like accumulations, and large round inclusions of ubiquitylated proteins), and found that the expression levels of all 4 genes were changed before all types of ubiquitylated protein accumulation (data not shown).

DISCUSSION

We demonstrated that *DCTN1*, *EGR3*, *ACATN*, *CCNC*, and *DR5* are differentially expressed in the residual motor neurons in sporadic ALS. Furthermore, the expression levels of these genes are differentially correlated with the levels of pathologic markers, the numbers of residual motor neurons, and the degrees of cytoplasmic accumulation of pNF-H and ubiquitylated protein, which are considered to reflect degeneration processes of motor neurons in sporadic ALS (5, 16–18, 22). These 5 genes were selected from those showing the most marked and specific altered expression levels among 4,845 genes that we had previously assessed in

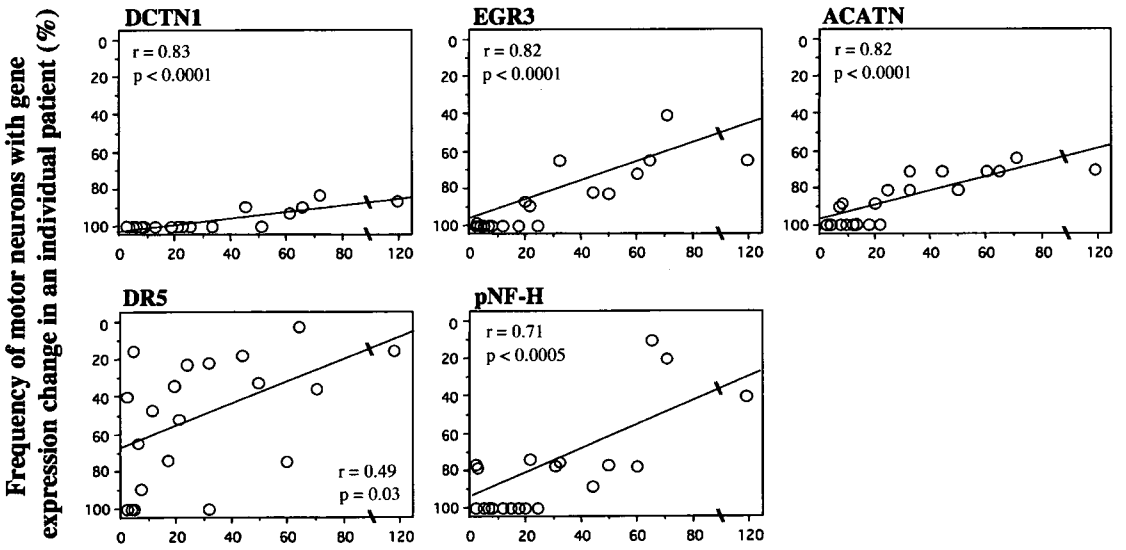

FIGURE 2. Frequency of motor neurons with gene expression change correlates with the extent of motor neuron loss. The correlation analyses between frequencies of motor neurons with gene expression changes (relative to controls) for *DCTN1*, *EGR3*, *ACATN*, *DR5*, and pNF-H and numbers of residual motor neurons were performed in the 20 patients with amyotrophic lateral sclerosis. The mean number of motor neuron patients in controls was 195 ± 17 (± SD) (range 176–225)/10 sections (n = 8). The values are inversely ordered on the y axis.

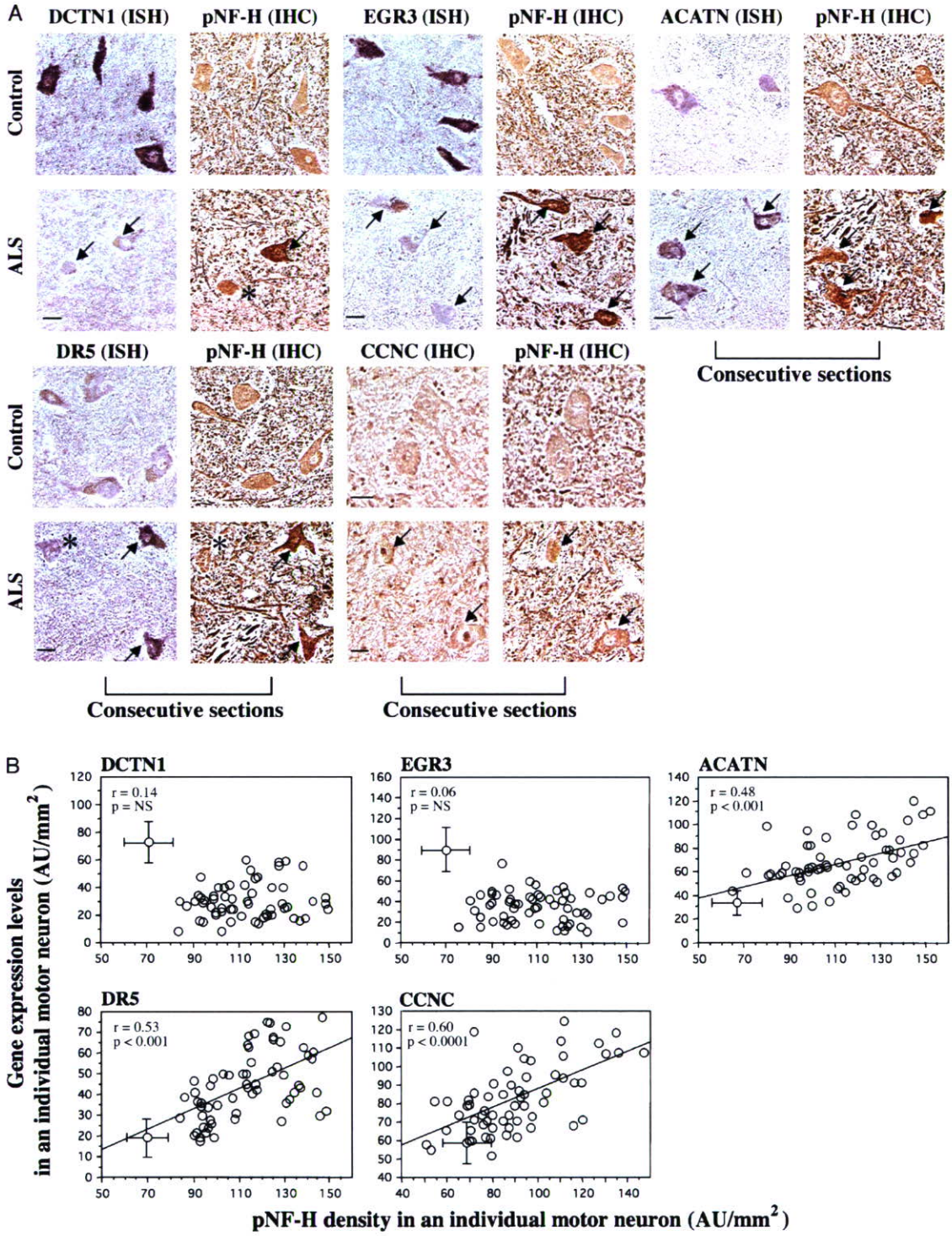

FIGURE 3. Gene expression and cytoplasmic phosphorylated neurofilament H (pNF-H) accumulation. **(A)** Gene expressions and pNF-H accumulation in identical motor neurons. Representative in situ hybridization (ISH) for *DCTN1*, *EGR3*, *ACATN*, and *DR5*, and immunohistochemistry (IHC) for CCNC are shown compared with pNF-H staining (IHC) on consecutive spinal cord sections from patients with amyotrophic lateral sclerosis (ALS) and control patients. The accumulation of cytoplasmic pNF-H was prominent in ALS motor neurons. Arrows denote motor neurons with gene expression or protein accumulation changes compared with control patients, and asterisks denote those with unchanged levels. Scale bars = 25 μm. **(B)** Expression levels of genes were compared with the level of pNF-H accumulation in individual motor neurons. Expression levels of *ACATN*, *DR5*, and CCNC were correlated with the accumulation of pNF-H, whereas those of *DCTN1* and *EGR3* were not. Consecutive transverse spinal cord sections were assessed from 8 representative patients with ALS. The control values for gene and protein expression levels and the accumulation of pNF-H are shown as means ± SD for 8 control cases. AU, arbitrary absorbance units; NS, not significant.

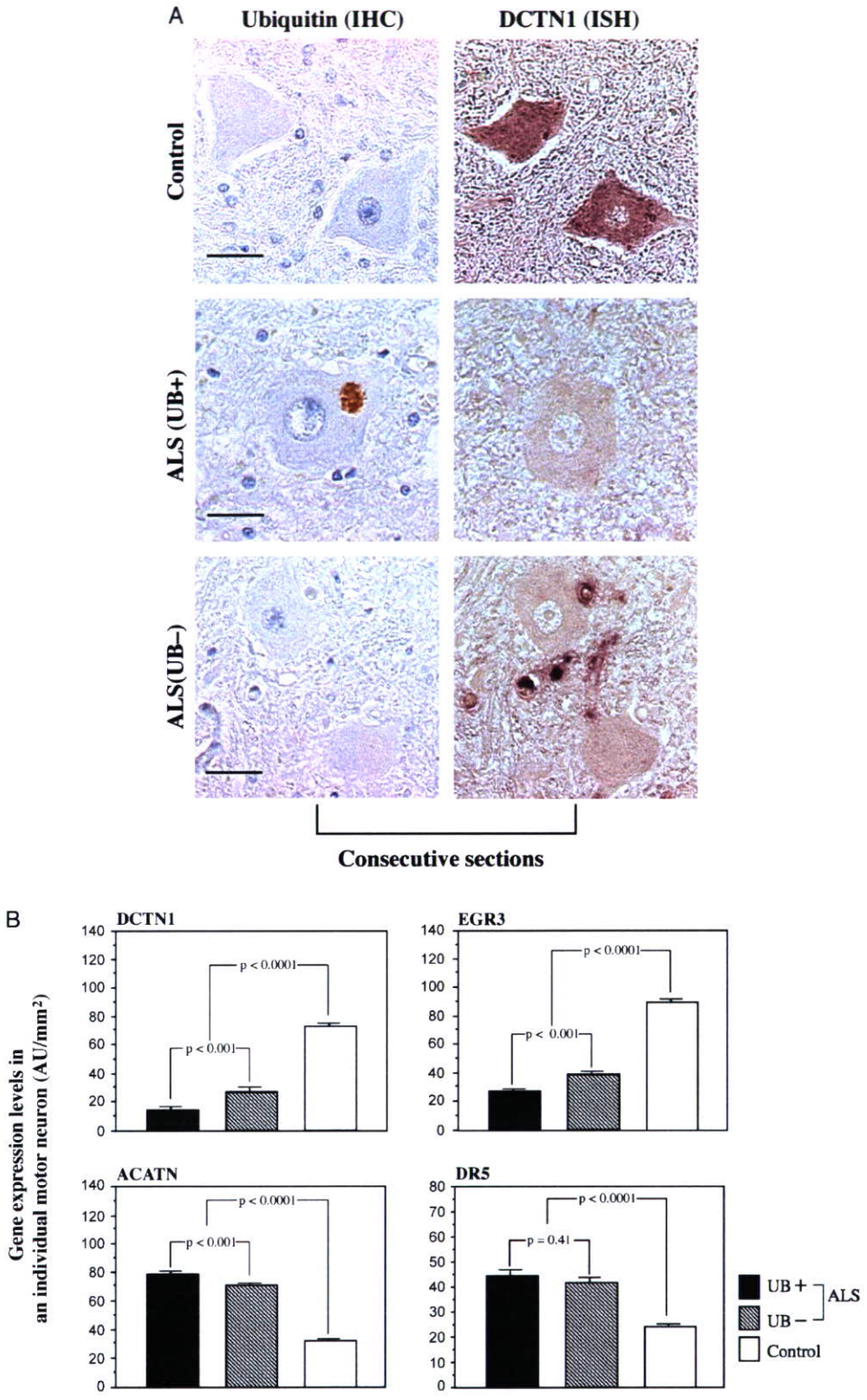

FIGURE 4. Gene expression and cytoplasmic accumulation of ubiquitylated proteins. **(A)** Representative *DCTN1* in situ hybridization (ISH) and ubiquitin (UB) immunohistochemistry (IHC) in identical motor neurons of consecutive sections are shown in patients with amyotrophic lateral sclerosis (ALS) and control patients. Scale bars = 25 μm. **(B)** Expression levels of genes were compared among the motor neurons that were either positive (n = 56) or negative (n = 175) for ubiquitylated proteins in 8 representative patients with ALS and those (n = 209) in 8 control patients. Expression levels of *DCTN1*, *EGR3*, and *ACATN* were significantly different in ubiquitin-positive compared to ubiquitin-negative neurons in ALS, whereas that of *DR5* was not. The values are shown as means ± SE. AU, arbitrary absorbance units.